

**REPUBLIC OF TURKEY
ISTANBUL GELISIM UNIVERSITY
INSTITUTE OF GRADUATE STUDIES**

Department of Electrical-Electronic Engineering

**DEVELOPMENT OF AN ALGORITHM FOR
RESTORATION AND ENHANCEMENT OF
ULTRASOUND MEDICAL IMAGING**

Master Thesis

AL HUSSEIN MYASAR M. SALIH AL-BAYATI

Supervisor

Asst. Prof. Dr. Musaria Karim MAHMOOD

Istanbul – 2022

THESIS PRESENTATION FORM

AUTHOR'S NAME : AL Hussein Myasar M. Salih AL-BAYATI
SURNAME

LANGUAGE OF THESIS : English

THESIS NAME : Development of an Algorithm for Restoration and Enhancement of Ultrasound Medical Imaging

INSTITUTE : Istanbul Gelişim University Graduate Education Institute

DEPARTMENT : Electric and Electronic Engineering

THESIS TYPE : Post Graduate

DATE OF THE THESIS : 30.05.2022

NUMBER OF PAGES : 52

THESIS ADVISORS : Asst. Prof. Dr. Musaria Karim MAHMOOD

INDEX TERMS : cardiac ultrasound imaging, anisotropic geodesic filter, Gaussian filtering .

TURKISH ABSTRACT : Tıp bilimi teknolojisindeki hızlı ilerleyen değişim, özellikle rekonstrüksiyon yöntemleri, bilimsel hayal gücü alanında da tıbbi tanıda en büyük avantajlara sahiptir. İster uzamsal ister frekans açısından büyücü temellerinin çeşitli alanlarında temel filtreleme teknikleri kullanılarak görüntü iyileştirme ve restorasyon için farklı yöntemler geliştirilmiştir. Günümüzde tıp pratisyenleri ve üreticileri için, teknoloji fiziksel sınırlarına ulaştıkça ultrason görüntü kalitesini iyileştirmek bir zorluktur. Ultrason görüntüleri, non-invaziv tanılama için çok yardımcıdır, ancak gölgeleme, sınırlı görüş alanı ve benek gürültüsü gibi çok çeşitli artefaktlardan muzdariptir. Bu çalışmanın ana odağı, kardiyak ultrason görüntülemeye yeni bir doğrusal olmayan görüntü işleme tekniğinin uygulanması ve daha spesifik olarak çarpımsal benek gürültüsünü azaltmak için çeşitli yöntemler üzerinedir. Geçmişte benek

gürültüsünü azaltmak için çeşitli filtreleme teknikleri önerilmiştir; ancak, benek paraziti azaltma ile görüntü özelliklerinin korunması arasında bir uzlaşmaya ulaşmak zor olduğundan performansları hala sınırlıdır. Bu çalışmada, kardiyak ultrason görüntülerinde çarpımsal gürültüyü azaltmak için anizotropik bir jeodezik filtreleme algoritması önerilmiştir. Algoritma, Gauss filtrelemeye benzer bir ölçek-uzay filtreleme tekniğine dayanmaktadır, ancak Gauss ağırlıklarının, kenarları otomatik olarak koruyabilen pikseller arasında doğrusal olmayan bir jeodezik mesafe hesaplaması kullanılarak otomatik olarak değiştirilmesidir. Araştırmada, önerilen anizotropik jeodezik filtre, Gauss filtresi, medyan filtresi ve gradyan tabanlı anizotropik difüzyona dayalı diğer doğrusal olmayan filtre türleri gibi çeşitli mevcut filtrelerle karşılaştırılmıştır. Önerilen anizotropik jeodezik filtrenin özellikleri koruma açısından en iyi performansı gösterdiğini ve aynı zamanda gerçek zamanlı 2D ve 3D eko-kardiyografilerin sinyal-gürültü oranlarında iyileştirmeler sağlayabileceğini gösteriyoruz. Sinyal-gürültü oranı (SNR), ortalama kare hata (RMSE), tepe sinyal-gürültü oranı (PSNR), kontrast oranı ve kontrast-gürültü oranını karşılaştıran gerçek dünya görüntülerinde, önerilen algoritma doğrusalır (CNR)

DISTRIBUTION LIST

1. Istanbul Gelişim University Graduate Education Institute
2. YÖK National Thesis Center

AL Hussein Myasar M. Salih AL-BAYATI

**REPUBLIC OF TURKEY
ISTANBUL GELISIM UNIVERSITY
INSTITUTE OF GRADUATE STUDIES**

Department of Electrical-Electronic Engineering

**DEVELOPMENT OF AN ALGORITHM FOR
RESTORATION AND ENHANCEMENT OF
ULTRASOUND MEDICAL IMAGING**

Master Thesis

AL HUSSEIN MYASAR M. SALIH AL-BAYATI

Supervisor

Asst. Prof. Dr. Musaria Karim MAHMOOD

Istanbul – 2022

DECLARATION

I hereby declare that in the preparation of this thesis, scientific ethics are complied with, in case the works of others are used, it is referred to in accordance with scientific norms, there is no alteration in the data used, and any part of the thesis / project is not presented as another thesis / project in this university or another university.

AL Hussein Myasar M. Salih AL-BAYATI

.../.../2022



**TO ISTANBUL GELISIM UNIVERSITY
THE DIRECTORATE OF INSTITUTE OF GDADUATE STUIES**

The thesis study of **AL Hussein MYASAR M. SALIH AL-BAYATI** titled as **Development of an Algorithm for Restoration and Enhancement of Ultrasound Medical Imaging** has been accepted as MASTER THESIS in the department of ELECTRICAL AND ELECTRONIC ENGINEERING by out jury.

Director

Signature

*Asst. Prof. Dr. Musaria Karim MAHMOOD
(Supervisor)*

Member

Signature

Asst. Prof. Dr. Mahmoud H. K. ALDABABSA

Member

Signature

Asst. Prof. Dr. AFM Shahan SHAH

APPROVAL

I approve that the signatures above signatures belong to the aforementioned faculty members.... / ... / 2022

Signature

Prof. Dr. Izzet GUMUS

Director of the Institute

SUMMARY

For many decades, the topic of medical imagery was of great interest. Diagnoses and care of the patient are important for mages in the medical profession. The restoration and improvement techniques of the medical magic have been widely explored and many questions remain unresolved. Different methods for image enhancement and restoration have been developed using basic filtering techniques in various domains of image fundamentals whether it is spatial or in terms of frequency. It is a challenge today for medical practitioners and manufacturers to improve ultrasound image quality as the technology has reached its physical limits. Ultrasound images are a great help for non-invasive diagnostics but suffer from a wide variety of artifacts such as shadowing, limited field of view, and speckle noise. The main focus of this study is on the application of a non-linear image processing technique in cardiac ultrasound imaging and more specifically on various methods to reduce multiplicative speckle noise. Various filtering techniques for speckle noise reduction have been proposed in the past; however, their performances are still limited as a compromise between speckle noise reduction and image features preservation is difficult to reach. In this study, an anisotropic geodesic filtering algorithm is proposed to reduce the multiplicative noise in CUIs. The algorithm is based on a scale-space filtering technique comparable to Gaussian filtering which automatically modified using a non-linear geodesic distance calculation between the pixels which is capable of automatically preserving edges. In the research, the proposed anisotropic geodesic filter is compared to various existing filters such as Gaussian filter, median filter. We demonstrate that the proposed anisotropic geodesic filter performs better in terms of preserving features and at the same time can provide improvements to the SNR of real-time 2D and 3D echo-cardiographs. In real-world images comparing SNR, RMSE, PSNR, contrast ratio, and contrast-to-noise ratio, the proposed algorithm is validated (CNR).

Keywords : Cardiac Ultrasound Imaging, Anisotropic Geodesic Filter, Gaussian Filtering.

ÖZET

On yıllar boyunca tıbbi görüntü konusu büyük ilgi gördü. Hastanın teşhisi ve bakımı, tıp mesleğindeki büyücüler için önemlidir. Tıbbi büyünün restorasyon ve iyileştirme teknikleri geniş çapta araştırıldı ve birçok soru çözülmeden kaldı. İster uzamsal ister frekans açısından büyücü temellerinin çeşitli alanlarında temel filtreleme teknikleri kullanılarak görüntü iyileştirme ve restorasyon için farklı yöntemler geliştirilmiştir. Günümüzde tıp pratisyenleri ve üreticileri için, teknoloji fiziksel sınırlarına ulaştıkça ultrason görüntü kalitesini iyileştirmek bir zorluktur. Ultrason görüntüleri, non-invaziv tanılama için çok yardımcıdır, ancak gölgeleme, sınırlı görüş alanı ve benek gürültüsü gibi çok çeşitli artefaktlardan muzdariptir. Bu çalışmanın ana odağı, kardiyak ultrason görüntüleme için yeni bir doğrusal olmayan görüntü işleme tekniğinin uygulanması ve daha spesifik olarak çarpımsal benek gürültüsünü azaltmak için çeşitli yöntemler üzerinedir. Geçmişte benek gürültüsünü azaltmak için çeşitli filtreleme teknikleri önerilmiştir; ancak, benek paraziti azaltma ile görüntü özelliklerinin korunması arasında bir uzlaşmaya ulaşmak zor olduğundan performansları hala sınırlıdır. Bu çalışmada, kardiyak ultrason görüntülerinde çarpımsal gürültüyü azaltmak için anizotropik bir jeodezik filtreleme algoritması önerilmiştir. Algoritma, Gauss filtrelemeye benzer bir ölçek-uzay filtreleme tekniğine dayanmaktadır, ancak Gauss ağırlıklarının, kenarları otomatik olarak koruyabilen pikseller arasında doğrusal olmayan bir jeodezik mesafe hesaplaması kullanılarak otomatik olarak değiştirilmesidir. Araştırmada, önerilen anizotropik jeodezik filtre, Gauss filtresi, medyan filtresi ve gradyan tabanlı anizotropik difüzyona dayalı diğer doğrusal olmayan filtre türleri gibi çeşitli mevcut filtrelerle karşılaştırılmıştır. Önerilen anizotropik jeodezik filtrenin özellikleri koruma açısından en iyi performansı gösterdiğini ve aynı zamanda gerçek zamanlı 2D ve 3D eko-kardiyografilerin sinyal-gürültü oranlarında iyileştirmeler sağlayabileceğini gösteriyoruz. SNR, RMSE, PSNR, kontrast oranı ve kontrast-gürültü oranını karşılaştıran gerçek dünya görüntülerinde, önerilen algoritma doğrulanır (CNR)..

Anahtar Kelimeler : kardiyak ultrason görüntüleme, anizotropik jeodezik filtre, Gauss filtreleme.

TABLE OF CONTENTS

SUMMARY	I
ÖZET	II
TABLE OF CONTENTS	III
ABBREVIATIONS.....	V
LIST OF TABLES	VI
LIST OF FIGURES	VII

CHAPTER ONE

INTRODUCTION

Introduction.....	1
1.1 General Overview.....	1
1.2 Background	2
1.2.1 Speckle Noise in Ultrasound Images	2
1.3 Literature Survey.....	3
1.4 Motivation	5
1.5 Problem Formulation.....	6
1.6 Research aims.....	6
1.7 Thesis Organization.....	7

CHAPTER TWO

THEORETICAL BACKGROUND

2.1 Medical Ultrasound Imaging.....	8
2.2 Ultrasound Diagnostic Characteristics	10
2.2.1 Acoustic Impedance.....	10
2.2.2 Acoustic Boundaries	10
2.2.3 Reflection of Ultrasound Waves	10
2.2.4 Refraction of Ultrasound Waves.....	11
2.2.5 Scattering of Ultrasound Waves.....	11
2.2.6 Absorption of ultrasound Waves.....	11
2.2.7 Beam divergence and Interference.....	11
2.3 Speckle Noise in Ultrasound Images	11
2.3.1 Types of Noise	12
2.3.2 Reduction of Speckle Noise.....	13
2.4 Filter	14
2.4.1 Wavelet Filter.....	14

2.4.2 Kuan Filter.....	14
2.4.3 Gamma Filter.....	15
2.4.5 Kalman Filter.....	15
2.4.6 Geometric Filter.....	16
2.4.7 Oddy Filter.....	16
2.4.8 Adaptive Surface Filter (ASF).....	17
2.4.9 Homomorphic Filter	17
2.5 Benchmark Filters	17
2.5.1 Gaussian Filter.....	17
2.5.2 Median Filter.....	18
2.6 A Geodesic Filter.....	18

CHAPTER THREE

METHODOLOGY

3.1 Proposed System Overview.....	19
3.2 Theoretical Modeling	20
3.3 Geodesic Filter Algorithm.....	21
3.3.1 Geodesic Distances or Geodesic Trajectories	21
3.3.2 Geodesics Trajectory Algorithm	22
3.4 Ultrasound Medical Imaging Restoration Process	23
3.5 Filtering a 3D and 2D Ultrasound Images.....	24

CHAPTER FOUR

EXPERIMENTS

4.1 The Dataset Images	25
4.2 2D Ultrasound Filtering Results.....	25
4.3 3D Ultrasound Filtering Results.....	31
4.4 Quantitative Analysis	42
4.4.1 Signal-to-Noise-Ratio	42
4.4.2 Root-Mean-Square-Error:	43
4.4.3 Peak-Signal-to-Noise-Ratio	43
4.5 Image Contrast Change	44
4.5.1 Contrast-to-Noise-Ratio:.....	44

4.6	Comparison Between the Four Algorithms.....	44
4.7	Discussion:	45

CHAPTER FIVE

CONCLUSION AND FUTURE WORKS

5.1	Conclusions	46
5.2	Future Works	47
REFERENCES		48



ABBREVIATIONS

1D	: One Dimension
2D	: Two Dimensions
3D	: Three Dimensions
4D	: Four Dimensions
ASF	: Adaptive Surface Filter
AR	: Autoregressive
CNR	: Contrast-To-Noise Ratio
CT	: Computed Tomography
CUI	: Cardiac Ultrasound Image
EEG	: Electroencephalography
GGD	: Generalized Gaussian Distribution
GPU	: Graphics Processing Unit
IC	: Image Contrast
MAP	: Maximum-A-Posteriori
MAX	: Maximum
MMSE	: Minimum Mean Square Error
MRI	: Magnetic Resonance Imaging
MSE	: Mean Square Error
NSHP	: Non-Symmetric Half Plane
PSNR	: Peak Signal-To-Noise-Ratio
PSNR	: Peak Signal to Noise Ratio

RF	: Radio Frequency
RMSE	: Root-Mean-Square-Error
SAR	: Synthetic Opening Radar
SNR	: Signal To-Noise-Ratio
SNR	: Signal To Noise Ratio
SS-SP	: Single Source Shortest Path
TGCD	: Think Gear Connector Driver
UDWT	: Undecimated Discrete Wavelet Transform
US	: Ultrasound
VCU	: Volunteer Cardiac Ultrasound

LIST OF TABLES

Table 2.1: Frequency range of an Ultrasound imaging	9
Table 4.1: Metrics Values for Noisy Image	45
Table 4.2: Metrics values for Gaussian filtering with variable sigma.....	45
Table 4.3: Metrics values for Median filtering with variable sigma.....	44
Table 4.4: Metrics values for AG with variable S; window size=3x3.....	44
Table 4.5: Metrics values for AG with variable S; window size=11x11.....	45



LIST OF FIGURES

Figure 1.1: Siemens ACUSON SC2000 image acquisition.....	2
Figure 1.2: Mathematical formulation of Noisy Image	3
Figure 1.3: Block diagram of the proposed filtering approach.....	7
Figure 2.1: Ultrasound technique for image acquisition	10
Figure 3.1: Block Diagram Of The Proposed Filtering Approach.....	22
Figure 4.1: Gaussian filter $S=1$	26
Figure 4.2: Gaussian filter $S=1.5$	26
Figure 4.3: Gaussian filter $S=2$	27
Figure 4.4: Median Filter $=1$	27
Figure 4.5: Median $S=1.5$	28
Figure 4.6: Median $S=1.5$	28
Figure 4.7: Proposed Filter Of VCU Image.....	29
Figure 4.8: Proposed filter with varying window size for volunteer CUI	31
Figure 4.9: Original Cardiac Phantom Ultrasound.	32
Figure 4.10: Proposed 3D Filter for The Cardiac Phantom Ultrasound $\sigma = 5$	33
Figure 4.11: Original VCU	34
Figure 4.12: Proposed 3D filter for VCU with $\sigma = 5$	35
Figure 4.13: Proposed 3D filter for VCU for windows size= 3×3	36
Figure 4.14: Proposed 3D filter for VCU for windows size= 5×5	37
Figure 4.15: Proposed 3D filter for VCU for windows size= 7×7	38
Figure 4.16: Proposed 3D filter for VCU for windows size= 11×11	39
Figure 4.17: Gaussian Filter-VCU image for $\sigma = 5$	40
Figure 4.18 : Median filter - VCU image for a window size of 5×5	41

CHAPTER ONE

INTRODUCTION

Noise is a common factor that affects the resolution of images causing blurring of fine and sharp details of the images. The occurrence of noises in the images is in general due to the physical nature of the imaging systems. Noises in the images can be broadly categorized into additive or multiplicative. Additive noises are easy to remove but multiplicative noises are image dependent, so it is complex to model and difficult to remove. Speckle is a multiplicative noise found in all coherent imaging systems. Medical ultrasound imaging known also as ultrasonography, is a coherent imaging technique widely used in medical applications like general abdominal imaging, obstetrics and gynecology, urology, cardiology, and as a guide in many surgical procedures. The images are generated by the pulse-echo technique with frequencies ranging from 1-20 MHz, Lopes, Nezry, Touzi, and Laur. (1990). Ultrasound waves are transmitted from the transducer into the region of interest and the reflection of these waves are detected by the same transducer and then will display. Echo signals resulting from the scattering and reflection are detected and then, the ultrasound waves are transmitted and displayed Perona P., Malik J. (1990).

1.1 General Overview

In medical image processing, noise reduction still remains a challenge for researchers and clinicians. Reliable image processing methods for Magnetic Resonance Imaging (MRI), X- Rays Scan tomography (CT), and ultrasound (US) are essential to improve the diagnostic analysis and compensate for instrumental artifacts. The quality of medical images is determined by a number of factors which originates from the physical phenomenon measured by the sensors and by the reconstruction algorithms Perona P., Malik J. (1990) and Lifeng Yu, Mayo Clinic, Rochester, Shuai Leng, (2016). The main challenge for developing different noise reduction techniques is to improve SNR without losing important clinical features in the image. Over the past decades, several image processing techniques focusing on reducing multiplicative ‘speckle’ noise prevalent in ultrasound imaging has been proposed. The system consists of a 2D ultrasound machine as shown in Fig 1.1.

Picture post-handling procedures don't need any kind of equipment changes and can be applied to both old and new picture informational indexes, Michailovich, O. V., Tannenbaum A. (2006). The compromise between the need to reduce multiplicative and additive noises in ultrasound images and the preservation of important image features represents a great challenge, which we will attempt to address in this thesis. Several techniques for reducing ultrasound multiplicative and additive noises have been developed in the past and a majority of these filtering techniques fall in one of the three categories - local algorithms, anisotropic based techniques, and wavelet-based methods.

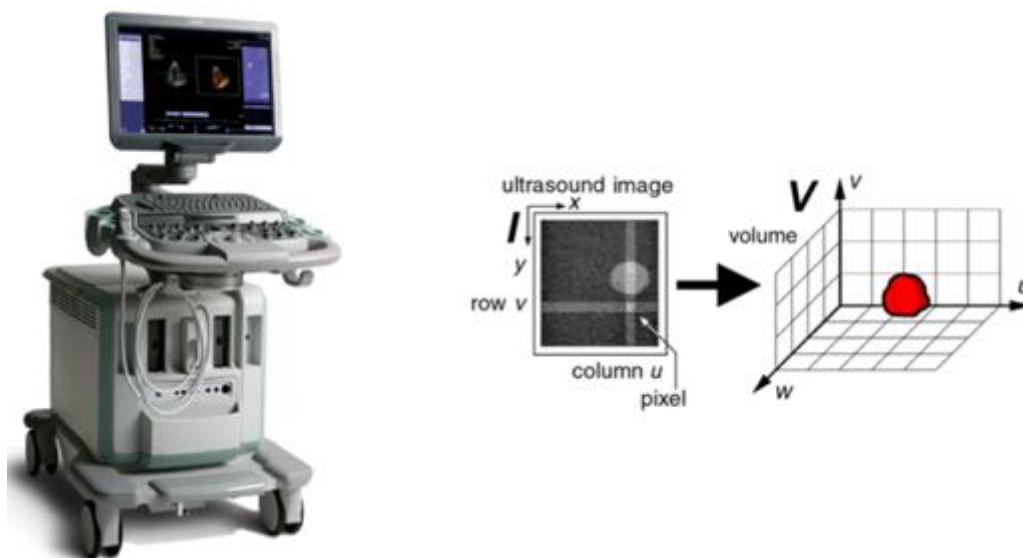


Fig. 0.1: Siemens ACUSON SC2000 image acquisition

1.2 Background

1.2.1 Speckle Noise in Ultrasound Images

Speckle noise is an impedance design found in a picture framed with sound radiation of a medium containing many sub-goals dissipates. Various rudimentary dissipates mirror the occurrence wave towards the sensor. The dispersed, coherent waves with different phases are randomly interfered with constructively or destructively. A random granular motif, the speckle, is the distorting effect on the interpretation of the content of the image.

Speckle noise is a peculiarity that goes with all sound imaging modalities wherein pictures are delivered by meddling reverberations of a communicated waveform that exude from heterogeneities of the concentrated-on objects. The superposition of acoustical reverberations accompanying arbitrary stages and amplitudes will in general create an unpredictable impedance

design, known as spot commotion, that scales from zero to a most extreme, contingent upon whether the obstruction is horrendous or valuable, Michailovich, O. V., Tannenbaum A. (2006).

Digital images contain various forms of noises including noise impulse, additional sound, and frequency noise. In general, speckle noises are generated because of the travelling path difference of the particular coherent acoustic waves that presents the interference. Speckle noises are quite different from other classical noises sorts such as impulse and Gaussian noises. It has a shape like the granular spot in the whole image space. The specific denoising techniques applied to remove impulse noise or Gaussian noises are not sufficient or de-speckling unless these methods are adjusted based on the characteristic of speckle noise. It is quite difficult for recognizing and extracting features of ultrasound imaging since this sort of noise is particularly being directly affecting the diagnostic value of the imaging form. Where the elimination of these noises is a primary target while analysing and observing the ultrasound images for significant disease characterization.

Though there is no any ideal solution for image noise issues, there are so many techniques available which can reduce/minimize image noise at desired level. So, image denoising is the process of removing/minimizing noise from a noisy image resulting from the superposition of both the clean/original image and the noisy-image component as in Fig. 1.2, S. Hariharasudhan and Dr. B. Raghu. (2016).

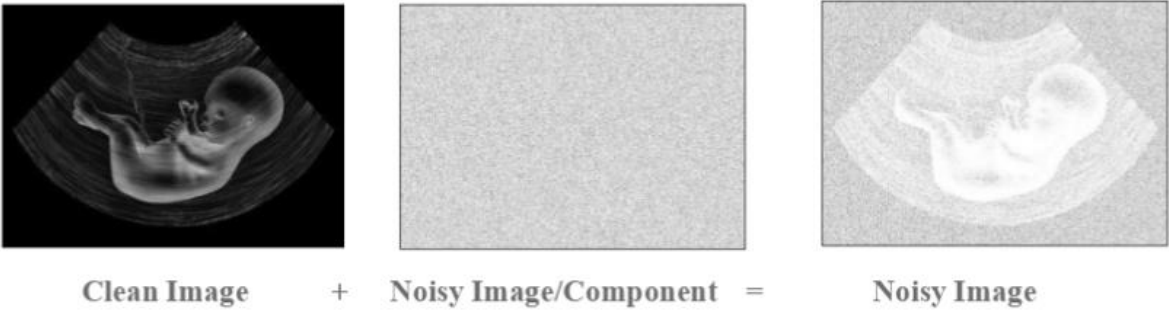


Fig. 0.2: Mathematical formulation of Noisy Image, Hariharasudhan S., and Dr. Raghu B.(2016)

1.3 Literature Survey

Speckle reduces the accuracy of ultrasound images and thus reduces a human observer's ability to discern fine diagnostic data. Speckle is not a picture sound, but a contrasting noise like shift. As discussed above, the speckle noise is basically a multiplicative noise when a sound wave pulse interferes on a sound wave-length scale spontaneous. Speckle sounds are characterized as multiple sounds, which is intrinsic to an ultrasound image with a granular pattern. Speckle is the

outcome of diffuse diffusion if an ultrasound pulse interferes at random, on a scale close to the sound wavelength, with tiny particles or artifacts.

The Speckle algorithms attempt to erase the spindle without losing the essential fine image characteristics. Most previous approaches to denoise ultrasound pictures are based on in adaptive and adaptive filters to be addressed in the next section. It is understood, however, that standard filtering methods in noise sometimes lead to boring images. Speckle noise images reduce the image contrast and make it hard to perform image processing operations such as border detection, segmentation etc.

The problem with photos losses is that unnecessary distortions must be reduced because of the presence of noise, or due to the poor image acquisition process, which adversely affects image analyses and the process of interpretation., Jing Bianca S. Gerendas Christian Simader Georg Langs Sebastian M. Waldstein Ursula Schmidt-Erfurth Ehsan Shahrian Varnousfaderani, Wolf-Dieter Vogl. (2016).

Speckle filters come from the community of the synthetic opening radar. These filters have been used since the early 1980s for ultrasound imaging. The work of reducing or suppressing speckle noise in ultrasound going on for a long time now.

Miscelled noise, based on various mathematical models, is eliminated using several methods. For example, one approach uses Multi-Look Processing to avoid the speckle noise in a single ultrasound scan by taking a view of several" Yao Zhang, Heng Xue, Mixue Wang, Nan He, Zhibin Lv, Ligang Cui. (2021) and Franceschi A. M, and Rosenkrantz A. B. (2017).

Besides, it is needed to utilize versatile and non-versatile sign channels (where versatile channels adjust their loads across the picture to the dot level, and non-versatile channels apply similar loads consistently across the whole picture). This filter excludes information from the current image, particularly information of high frequency including fine anatomical characteristics. Adaptive filtering in high-texture areas improvement at the preservation of edges and detail. Non-adaptive filtering is easier to apply and less computer power is required, but unfortunately many essential fine structures are eliminated. Yao Zhang, Heng Xue, Mixue Wang, Nan He, Zhibin Lv, Ligang Cui. (2021) and Franceschi A. M, and Rosenkrantz A. B. (2017).

Using the wavelet transformation recently led to important progress in ultrasonic filtering. The key explanation for the use of multi-scaling processing is that many natural signals are greatly streamlined and modelled by established distributions when broken down into wavelet bases. In addition, the decomposition of a wavelet is possible at various scales and directions to distinguish noise and signal. The original signal can therefore be restored at all levels and directions and valuable information is not lost.

The first methods for multi-scale wavelet reduction based on detailed sub-band coefficient thresholds. The basis for these algorithms is the observation that in each spectral band (VW, WV, WW blocks) the wavelet coefficients (almost nil) and R covariance matrix can be modelled as a two-normal median distribution ($V_x; v_y$) (real and imaginary parts are correlated). Furthermore, each block normally has a differently directed distributions. In light of this reality, a calculation that performs wavelet coefficients thresholding concerning the chief tomahawks of the 2-D appropriations, Mathew K., Shibu S. (2014) and Hongga Li, Bo Huang, Xiaoxia Huang, (2010).

Unfortunately, wavelet algorithms suffer from many limitations which makes their use in ultrasound image processing difficult.

- The threshold is chosen ad hoc, so that signal and noise elements, irrespective of their size and orientation, are known to their distributions.;
- The threshold technique usually results in the de-noised picture of certain objects.;
- Non-linear estimators based on Bayes theory were designed to solve these issues.;

Several authors in literature have suggested various ways of solving this dilemma. One approach involves transforming picture signals with Gaussian in-creasing (size) kernels and then evaluating the evolution of signal functions along the scale. Adaptive smoothing was suggested to facilitate the analysis of scale-space representations rather than gaussian smoothing. The general principle behind adaptive smoothing is to use various kernels with supports and shapes depending on the local properties of the signal to be smoothed. In Palwinder Singh, Leena Jain. (2013) and Noor H. Resham, Heba Kh. Abbas, Haidar J. Mohamad, Anwar H. Al-Saleh (2021) a description of the adaptive filters.

1.4 MOTIVATION

As reviewed in this chapter there are several adaptive filters in literature which are proposed to achieve a better result by varying window size and also preserve the feature like edges. Filters that have adaptive nature include Lee, Frost, Kuan, Enhanced Frost, and Enhanced Lee filter Lopes, Nezry, Touzi, and Laur. (1990). One of major problems in applying all of these algorithms to ultrasound image analysis is that the weight used to compute the pixel similarities in a neighbourhood are all based on ad-hoc functions. Therefore, linear methods with fixed weights are not suitable in the kernel because it assumes that the neighbouring pixels come from a smooth distribution where only geometric distance from the central pixel is important. A convolution kernel with locally determined coefficients is required for a non-linear geodesic distance transform that measure the true distance between the central pixel with its neighbours

in space and in intensity, which is the basis of this work. The presence of the speckle noise is the biggest problem in ultrasound imaging. Speckle noise has a negative effect on the images' quality because the pattern of the speckle does not correspond to the organ structure underlying the photograph. Speckle noise is responsible in comparison with other imaging options for the poorer resolution of an ultrasonic image. Speckle reduction has therefore become an active research field. To compensate for such data corruption, it is very important to use an effective denoising technique.

1.5 Problem Formulation

The accurate and effective human interpretation and computer assisted analysis of many imaging modalities is often dependent on the image quality and operational experience. Interpretation of ultrasound images requires special training and experience. Due to strong artifacts in the ultrasound image by speckle noise, even experienced sonographers cannot make a confident diagnosis from the images. Speckle is a textured appearance that is caused by small, tightly spaced structures, too small for the point diffusion function to solve. Speckle noise generally does not reflect the underlying tissue structure. The regional mean texture luminosity reflects the tissue's regional echogenicity. The presence of speckle noise has severely degraded the image quality in applications such as visualization image and auto segmentation. In order to improve visualization and texture recovery in the picture, the speckle reduction filters were developed. Removal of texture increases automated object detection speed and accuracy. The main objective of this research work, is to design an efficient diffusion filter to enhance the details of the image by suppressing the speckle noise while preserving the edge details in the ultrasound images

1.6 Research Aims

The main contributions of the thesis are:

- 1.The development of a filter capable of reducing additive and speckle (multiplicative) noises in 2D and 3D ultrasound images without losing the localization of important features;
- 2.The ability to create a multi-resolution scale space where edge localization is preserved by using an efficient algorithm to compute geodesic distances;
- 3.A quantitative comparison of the performance of the geodesic filter with two of the most popular filters found in the literature namely: Gaussian, median.

1.7 THESIS ORGANIZATION

The thesis is organized as follows. Chapter 2 reviews the theoretical background of ultrasound imaging as well as the physics of ultrasound image formation and the various type of noises found in those images. Chapter 3 describes the proposed method for Cardiac Ultrasound Image (CUI) using Geodesic algorithm. Chapters 4 discusses the qualitative and quantitative comparison with two of the most popular filters found in the literature. In Chapter 5, we conclude the thesis with the analysis of the pros and cons of the geodesic filter to perform speckle reduction in ultrasound images and discuss some possible future works and improvements.



CHAPTER TWO

THEORETICAL BACKGROUND

This chapter presents a brief history of ultrasound imaging and discusses the different noise types associated with this modality as well as various techniques used to reduce its effect. Out of the numerous filters one can find in the literature, we will review the filters that will be used for the comparison with the proposed geodesic filter.

2.1 MEDICAL ULTRASOUND IMAGING

Ultrasonography displays the cross-sectional view of the object being scanned. The essential activity is the transmission of high recurrence sound waves into the body, trailed by gathering, handling and parametric showcase of reverberations getting back from the organs and tissues inside the body. This imaging strategy has become famous, as it is compact, and creates pictures with great goal without the utilization of ionizing radiation in a savvy way. This is a minimally invasive technique, and is very useful in the diagnosis of obstetrics. It is used to image the internal organs like heart, liver, gallbladder, spleen, kidney and to detect problems with muscles, tendons, ligaments, joints and soft tissue. Since ultrasonic imaging is real time, it demonstrates the movement of internal organs, tissues, and blood flow and heart valve functions. Ultrasound images are used to identify the presence of cysts, tumours, and fluid filled sacs. They are also used to examine the superficial structures in the body. The operating frequencies for typical application of the ultrasound imaging are listed in Table.2.1. High frequency waves cannot penetrate deeply and thus it is used in imaging superficial organs. Low frequency waves penetrate into the body, to image the deeply seated organs.

The fundamental limit of ultrasound imaging framework is the presence of spot commotion in the picture. Dot commotion is signal ward clamor, that emerges because of the obstruction of sent and reflected ultrasound waves in the locale of interest. Spot design is a type of multiplicative clamor and it relies upon the idea of the tissue being imaged, and different imaging boundaries.

Table 0.1. Frequency range of an Ultrasound imaging

Typical Application	Operating Frequency Range (MHz)
Cardiology, Obstetrics, Abdominal imaging	2 - 5
Ophthalmology, Peripheral Vascular imaging, Testicular imaging	10 -20
Intra-arterial imaging	20 - 50

Speckle noise degrades the detecting ability of the target and reduces the contrast and resolution of the ultrasound image. This affects the human ability to identify the difference between a pathological tissue and a normal tissue. Bamber & Draft (1980) had suggested that the speckle noise reduces the detecting ability of the lesion by a factor of eight. Hence the main objective of this thesis is to address the problem of speckle noise reduction in the Ultrasound images.

Ultrasound is non-invasive imaging modality and one of the most inexpensive tools used for qualitative and quantitative assessments of patient's conditions. Ultrasound imaging technology is constantly and rapidly changing, ranging from cardiac imaging to pre-natal assessment. The use of ultrasound for medical imaging application is advantageous because it is safe to use, non-invasive in most applications and the image acquisition is real-time. Ultrasound imaging uses ultrasound waves produced from piezoelectric transducers that travel through the body tissues and/or organs which are then reflected back to receptors which turns ultrasound vibrations into electrical pulses where they are processed to compute the location of the reflected wave using time-of-flight. These transducers arrays are organized as 1D arrays or 2D arrays which produce respectively 2D or 3D images as in Figure 2.1, Lopes, Nezry, Touzi, and Laur. (1990). In general, the resolution of an ultrasound image varies with the number of elements in the transducer array and with the frequency of the ultrasound transducer used. In general, higher time resolution can be achieved when higher ultrasound frequencies are used but higher frequencies attenuate or are absorbed, faster than lower frequencies limiting the ability to observe deeper anatomical structures. Hence, there is a fundamental physical limit between time resolution and depth penetration. In addition, other artifacts can be created by the loss of proper contact or a gap between the transducer probe and the body. This can be solved by using impedance adaptive gel that reduces the reflection of the ultrasound from the contact between air and skin.



Fig. 0.1: Ultrasound technique for image acquisition

2.2 Ultrasound Diagnostic Characteristics

2.2.1 Acoustic Impedance

In a medium, the sound impedance (Z) may be defined as the product of medium density and ultrasound velocity of the medium. The degree to which the medium particles resist a change due to mechanical disturbances differs in various media, Hariharasudhan S., and Dr. Raghu B. (2016).

2.2.2 Acoustic Boundaries

Acoustic boundaries are tissue positions in which the value of acoustic impedance changes in tissue interactions during ultrasound interactions. The unique characteristics of diagnostic ultrasounds are based on the nature and spread of acoustic limits within the body's tissues.

2.2.3 Reflection of Ultrasound Waves

When an ultrasound beam hits an acoustic border, some of the energy in the beam is transmitted across the border and reverse or reflected. Depending on the size of the boundary, two kinds of reflection can occur. These reflections are specular and non-specular. The limits are smooth and larger than the dimension of the beam when the interface is smaller than the dimension of the beam, with special reflections.

2.2.4 Refraction of Ultrasound Waves

Refraction is a change of direction of the beam at the border between two media at different speeds. The wavelength of the ultrasound is changed, while the frequency of the beam remains unchanged, between the first and the second medium. $\text{speed} = \text{frequency} \times \text{wavelength}$, when the speed changes to the frequency value, the wavelength changes.

2.2.5 Scattering of Ultrasound Waves

The incident beam is reflected in many different directions when the reflecting interface is irregular in form, and its dimensions are smaller than the diameter of the ultrasound beam. This is called dispersion. The direction of dispersion depends on the relative dimensions of the dispersion target and the ultrasound beam diameter. The dispersion rises rapidly as the ultrasound frequency increases, Hariharasudhan S., and Dr. Raghu B. (2016).

2.2.6 Absorption of ultrasound Waves

Absorption is the process through which energy is transferred to the spreading medium in the ultrasound beam where it is converted into heat power. The medium absorbs energy from the beam and is affected by the medium's viscosity, the relaxing time and the frequency of the beam.

2.2.7 Beam divergence and Interference

Divergence of the ultrasound beam is defined as the spread of beam energy when moving away from the source while ultrasound interference refers to how the wave fronts interact. The intensity of the beam is affected axially as well as laterally (along the beam direction) (perpendicularly to the beam direction). Stressing or weakening the wave results. Interference. The dimensions and the way they differ have a great influence on image resolution in ultrasound diagnosis.

2.3 SPECKLE NOISE IN ULTRASOUND IMAGES

Speckle noise is a pattern of interference in an image that contains a consistent radiation medium that contains many scatters in sub resolution. A number of basic dispersions mirror the sensor wave incident. The dispersed, coherent waves with different phases are randomly interfered with constructively or destructively. A random granular motif, the

speckle, is the distorting effect on the interpretation of the content of the image. Blister noise in B-scan image degrades the target detection and reduces contrast, which affects the human ability to identify normal and pathological tissue. It also reduces the speed and accuracy of image processing ultrasound tasks such as segmentation and recording, Jing Bianca S. Gerendas Christian Simader Georg Langs Sebastian M. Waldstein Ursula Schmidt-Erfurth Ehsan Shahrian Varnousfaderani, Wolf-Dieter Vogl. (2016).

2.3.1 Types of Noise

Digital images contain various forms of noise. These include noise impulse, additional sound, frequency noise and a range of noises. There may be an impulse noise on one aspect of the sensor and on the loss of a signal. In this case, the picture is too high or too low for outlines. Wide-band adding noise comes from many natural causes, including thermal atomic vibrations in conductive systems, shot noise, black body, and amplifier changes. Additive noise follows simple statistical models such as Gaussian or normal distributions, and its effect can be reduced with linear filters. Frequency noise is characterized by the interference of a signal at specific frequencies, for example, 60 Hz noise created by the interference of a house electrical system with an instrument. Multiplying noise is a random signal that is unwanted, which multiplies by a signal. For ultrasound imaging, speckle noise is multiplicative. In most ultrasound images, we have a combination of additive and multiplicative noises.

2.3.2 Reduction of Speckle Noise

Speckle reduces the accuracy of ultrasound images and thus reduces a human observer's ability to discern fine diagnostic data. Speckle is not a picture sound, but a contrasting noise like shift. As discussed above, the speckle noise is basically a multiplicative noise when a sound wave pulse interferes on a sound wave-length scale spontaneous. Speckle sounds are characterized as multiple sounds, which is intrinsic to an ultrasound image with a granular pattern. Speckle is the result of diffuse spreading, when an ultrasound pulse interferes at random, on a scale close to the sound wavelength, with tiny particles or artifacts.

Dot decrease calculations attempt to eliminate the dot without annihilating the significant fine picture highlights. A large portion of the past methodologies for de-noising ultrasound pictures depend on non-versatile and versatile sifting strategies that will be examined in the following segment. In any case, it is notable that standard clamor sifting techniques regularly bring about obscured picture highlights. Pictures with dot commotion will bring about

diminishing the difference of a picture and make it hard to perform picture handling activities like edge identification, division, and so on.

The problem of image smoothing consists of reducing unwanted distortion due to the noise or poor image acquisition process that adversely affects the analysis and interpretation of images, with the preservation of important characteristics, including homogenic areas, discontinuities, edges, and textures, Jing Bianca S. Gerendas Christian Simader Georg Langs Sebastian M. Waldstein Ursula Schmidt-Erfurth Ehsan Shahrian Varnousfaderani, Wolf-Dieter Vogl. (2016). Filters that reduce speckles originated in the community of the synthetic opening radar (SAR), J. S. Lee, L. Jurkevich, P. Dewaele, P. Wambacq, A. Oosterlinckm, (2009). Those filters have been applied since the early 1980s to ultrasound imaging. Long work is being done now to reduce or suppress ultrasound spatula noise.

Two principal channel arrangements, to be specific single-scale spatial channels and change multi-scale space channels, have been created. The spatial channel is utilized to flush a picture; in other words, it decreases the variety in power between neighboring pixels. The straightforward sliding window spatial channel replaces the middle worth of the window by the normal of all the close by pixel esteems. It replaces, in this manner, pixels which are not agent of their current circumstance. It is normally completed with a convertible cover that ascertains another worth as a weighted amount of pixel and its neighbors' esteems for the focal plexin. On the off chance that the coefficients of the veil standardized to one, the normal brilliance of the picture won't change.

Several methods are used, based on various mathematical models to eliminate speckles of noise. One way for example is by using multiple looks, which means by taking a couple of "views" in a single ultrasound Yao Zhang, Heng Xue, Mixue Wang, Nan He, Zhibin Lv, Ligang Cui. (2021) the speckle noise, averages. The average of the views is the incoherent, Franceschi A. M, and Rosenkrantz A. B. (2017)

This filters also remove actual image information, especially high-frequency information such as fine anatomical characteristics. Adaptive sprocket filtering in high-texture areas is better for preserving edges and detail. Non-adaptive filters are easier to apply and require less computer power, but sadly remove many important fine structures, Franceschi A. M, and Rosenkrantz A. B. (2017).

Two non-adaptive forms of spring filtration are available: one based on moving mean and one based on the median (within a given rectangular window centered at a pixel). The medium filter better preserves the edges when noise spikes are eliminated, than move the average filter

like the Gaussian. The Lee filter, Frost filter and Maximum-A-posteriori (RGMAP) filter include numerous types of adaptive speckle filters. In their mathematical models they all base on three fundamental assumptions.

2.4 Filters

2.4.1 Wavelet Filter

The utilization of wavelet change has as of late prompted significant advancement in ultrasound separating. The primary justification for the utilization of multi-scale handling is that a considerable number of normal signs can be altogether worked on when deteriorated into wavelet puts together and demonstrated with respect to known disseminations. Besides, the wavelet breakdown can isolate sign and commotion on various scales and directions. The first sign can in this manner be recuperated on any scale and heading and valuable data isn't lost.

The first methods of multi-sized wavelet reduction were based on detailed sub-band coefficients thresholding, Hongga Li, Bo Huang, Xiaoxia Huang (2010). These algorithms are based on observation which indicates that wavelet coefficients in each spectral band can be modeled on a bi-normal ($V_x; V_y$) (nearly zero) and covariance R (normally not diagonal) distribution of mean ($V_x; V_y$) (real and imaginary parts are correlated). Moreover, distributions in each block are normally oriented differently. Therefore, an algorithm performs a threshold of wavelet coefficients for the main axis of 2-D distributions. Sixin Zhang, Stéphane Mallat (2021) and Hongga Li, Bo Huang, Xiaoxia Huang (2010).

2.4.2 Kuan Filter

This filter is used primarily to suppress speckle. It smooths image data without removing edges or sharp features in the images while minimizing the loss of radiometric and textural information. The Kuan filter first transforms the multiplicative noise model into a signal-dependent additive noise model. Then the minimum mean square error criteria is applied to the model. The resulting gray-level value (R) for the smoothed pixel is:

$$R = (I_c * W) + (I_m * (1 - w)) \quad (2.1)$$

where:

- $W = \frac{1 - Cu^2}{1 + Cu^2}$
- $Cu = \frac{1}{\text{Number of looks}}$
- $Ci = \frac{S}{I_m}$

- I_c =Center pixel in the kernel
- I_m =Mean value of intensity within the kernel
- S =standard deviation of intensity within the kernel

2.4.3 Gamma Filter

A filter based on a Bayesian analysis of the image statistics is a Gamma filter, Palwinder Singh, Leena Jain (2013). This assumes the Gamma distribution is based on both scene reflection and speckle noise. The "overlay" of these distributions produces a K-distribution that is known to match many radar return distributions. α is gamma filter parameter The estimate x is given by:

$$\hat{x} = \frac{(\alpha-L-1)\bar{y} + \sqrt{\bar{y}^2(\alpha-L-1)^2 + 4\alpha L y \bar{y}}}{2\alpha} \quad (2.2)$$

$$\alpha = \frac{L+1}{L(\sigma_y/\bar{y})^2 - 1} \quad (2.3)$$

2.4.4 Forst Filter

The Frost Filter is a versatile Wiener Filter which convolves the pixel esteems inside a decent size window with a dramatic drive reaction m given by:

$$m = \exp[-KC_y(t_0)|t|] \quad C_y = \frac{\sigma_y}{\bar{y}} \quad (2.4)$$

Where K is a channel boundary, t_0 shows the place of the pixel handled and $|t|$ the separation from pixel t_0 . is estimated. This answer comes from an autoregressive outstanding model expected for the scene x , Noor H. Resham, Heba Kh. Abbas, Haidar J. Mohamad, Anwar H. Al-Saleh (2021).

2.4.5 Kalman Filter

A 2D Kalman channel has been carried out on a causal expectation window, the supposed Non-Symmetric Half Plane (NSHP). In this channel, the picture is thought to be addressed by a Markov Field which fulfills the causal autoregressive (AR) model Lopes, Nezry, Touzi, and Laur. (1990).

$$x(m, n) = \sum_{(p,q) \in W} a_{pq} x(m - p, n - q) + u(m, n) \quad (2.5)$$

where $x(m, n)$ addresses the pixel esteem at area (m, n) , $u(m, n)$ is a clamor grouping (this isn't the spot commotion) which drives the Markov interaction and a_{pq} are the reflection coefficients of the autoregressive model. The boundaries a_{pq} are assessed in view of the worldwide evaluations of the autocorrelation grouping of the picture over the limited window W . The AR model for Kalman filter equations is arranged from these parameters into a recursive 2D block form. This filter is very involved and we are referring to the 2D cinematic model for further data and the Kalman filter equation (which is limited here to speckle modelling), Lopes, Nezry, Touzi, and Laur. (1990).

2.4.6 Geometric Filter

The geometric filter is a morphological nonlinear filter that uses the graphic concept. The graph is obtained through the transformation of the original picture into a 3D diagram, in which pixel cords indicate the pixel's position in the plane and the pixel value specifies the pixel height for that plane. The filtering process is first conducted with an 8-hulling algorithm on line segments of the image graph. Slice pixels are set to 1 when pixels are on or lower than the image graph surface, whereas pixels are set to 0. This algorithm scans for 4 different configurations and, when found one, the pixel of the graph that matches the main pixel for a mask shall be set to 0. The filtering algorithm scans 4 different configurations. For additional graphs and masks the procedure is repeated except that the central pixel is increased by 1. On columns and diagonal slices, the entire procedure is repeated. The geometric filter completes an iterative step. A filtering is made because speckles appear on the binary slice images like narrow walls and valleys and the geometric filter gradually fills and tears down these features through iterative repetition.

2.4.7 Oddy Filter

The Oddy filter can be considered as a mean filter whose window shape varies according to the local statistics Patel B. C., Sinha G. R. (2014). This filter is the closest to the one proposed in this thesis. The estimate \hat{x} is given by:

$$\hat{x} = \bar{y} \text{ if } m < \alpha \bar{y} \quad \hat{x} = \frac{\sum_k \sum_l W_{kl} y^{(k,l)}}{\sum_k \sum_l W_{kl}} \text{ if } m > \alpha \bar{y} \quad (2.6)$$

$$W_{kl} = 1 \text{ if } |y(k, l) - \bar{y}| < m \quad W_{kl} = 0 \text{ otherwise} \quad (2.7)$$

where \hat{x} is evaluated locally over a 3×3 window, $|$ and α is the filter parameter. W plays the role of an adaptive binary mask that is applied over the window.

2.4.8 Adaptive Surface Filter (ASF)

The Adaptive Surface Filter is known as the ASF filter Gravel P., Beaudoin G., De Guise, J. A. (2004). The concept of the local emerging surface is another adaptive mask filter. The l.e.s. is the area defined over the window of the image graph surface. For the 9 binary masks, the l.e.s. is calculated. The mask with a minimum l.e.s. is chosen and a medium filtering over the mask pixels is performed. A central pixel of the 5 - 5 window assigns the mean value.

2.4.9 Homomorphic Filter

Multiplicative clamor is considered in ultrasound pictures. This makes holes in past strategies as they are basically used to dispense with the added substance irregular commotion. Accordingly, a legitimate logarithmic change appears to happen on the first picture, which makes spot commotion added substance as displayed in the accompanying fairness:

$$\log[f(x, y, z)] = \log[g(x, y, z)] + \log[\eta(x, y, z)] \quad (2.8)$$

We now have an image that can be processed through traditional methods without multiplying noise. We can choose from various options at this point, one of the most common being the use of different convolution filters. In order to compare the proposed algorithm to the most common filters in the homomorphic context we will review: Gaussian filter, median filter. A description of each filters follows.

2.5 Benchmark Filters

2.5.1 Gaussian Filter

Gaussian is a filter that has a Gaussian function as an impulse (or an approximation to it). As it is expanded (standard deviation), the Gaussian has the special capacity to not make any more current arcades. This property permits the expulsion of edges that address different degrees of detail. The quantity of feeble and bogus edges separated is diminished by an expanding scale. This, notwithstanding, makes edges shift from their real or genuine position and the size of the Gaussian channel as well as the power conveyances behind that picture rely upon the edge's shift. The Gaussian channels numerically alter the information signal through a Gaussian capacity (the bit in light of the typical conveyance bend) that produces great outcomes in sound decrease and picture smoothness. The 2D form with the standard deviation σ for picture $I(x, y)$ of the Gaussian appropriation is given:

$$Gauss[I(x, y)] = \frac{1}{\sigma\sqrt{2\pi}} \exp - \frac{(x^2+y^2)}{2\sigma^2} \quad (2.9)$$

2.5.2 Median Filter

An intermediate filter is a strong, non-linear filter. It is mainly used in the photographic application that changes the average value of the image intensity where the distribution of spatial noise within the picture is not symmetrical and also eliminates pulses and spike noise, Jing Bianca S. Gerendas Christian Simader Georg Langs Sebastian M. Waldstein Ursula Schmidt-Erfurth Ehsan Shahrian Varnousfaderani, Wolf-Dieter Vogl. (2016). Median filter is similar to the averaging filter except that the center pixel is replaced by the median value of all pixels in the window neighborhood. Due to one of its properties, it is used to reduce impulse noise. Its main advantage is it preserves edges localization. Its main disadvantage is that extra time is needed for computation of the median value by sorting N pixel in the window.

2.6 A Geodesic Filter

Define an image I as the mapping:

$$I : (x, y) \rightarrow (I^1(x, y), I^2(x, y), \dots, I^n(x, y)) \quad (2.10)$$

where n is the number of channels. We can now introduce the matrix G is as positive semidefinite, since it is symmetric and all its principal minors are non-negative. Hence both its eigenvalues λ_1 and λ_2 are non-negative. These eigenvalues contain information about the multichannel gradients of the image.

Distances on orthogonal domain can be computed by solving an eikonal equation with appropriate boundary conditions:

$$|\nabla T(x, y)| = \lambda 1(x, y) \quad (2.13)$$

In order to preserve the edges in the filtering process, we propose to define the kernel function κ as a function of the geodesic distance between two points on the domain.

The eikonal equation in (2.13) has to be solved once for every pixel in the image in order to compute geodesic distances to the neighbours within the filter window, S. Di Zenzo, (1986).



CHAPTER THREE

METHODOLOGY

An approach to perform noise filtering for speckle reduction on 2D and 3D ultrasound images using an anisotropic geodesic filter is proposed. Anisotropic geodesic filtering is a Gaussian like filter, where as opposed to standard Gaussian filtering with fixed weight values are used, the weights are determined dynamically. In this scheme each convolution window is different and can adapt to local intensity and geometry variations. As will be demonstrated, this category of filter can preserve the localization of fine structures automatically without prior knowledge of the locations of intensity discontinuities and without the need to compute gradients like in Perona's algorithm Yao Zhang, Heng Xue, Mixue Wang, Nan He, Zhibin Lv, Ligang Cui. (2021). The filter is an application of an older concept developed during Boulanger's PhD thesis, Piotr Osinski, Jakub Markiewicz, Jarosław Nowisz, Michał Remiszewski, Albert Rasiński and Robert Sitnik.

3.1 Proposed System Overview

This study proposes an approach to perform noise filtering for speckle reduction on 2D and 3D ultrasound images using an anisotropic geodesic filter. Anisotropic geodesic filtering is a Gaussian like filter, whereas opposed to standard Gaussian filtering with fixed weight values are used, the weights are determined by the local geodesic distances computed from the cumulative spatial and intensity distances of the neighbouring pixels with the centre pixel inside a convolution window. In this scheme each convolution window is different and can adapt to local intensity and geometry variations. As will be demonstrated, this category of filter can preserve the localization of fine structures automatically without prior knowledge of the locations of intensity discontinuities and without the need to compute gradients like in Perona's algorithm Perona P., Malik J. (1990).

3.2 Theoretical Modeling

It is not an easy task to filter volumetric ultrasound data since it is contaminated by additive and multiplicative noises at the same time. Speckle is basically a form of multiplicative noise that displays a granular pattern caused by the transducer. The distribution of speckle noise in ultrasound images has been largely studied in the literature and many models have been proposed. In this research, we use the noise model proposed by Mohammad Ashraful Islam, Rafid Mostafiz, Mithun Kumar PK, Mohammad Motiur Rahman (2018), which is the most

widely accepted recently, and has been successfully used in many studies. The noise model is the following:

$$f(x, y, z) = g(x, y, z) \times \eta(x, y, z) + \beta(x, y, z) \quad (3.1)$$

where $f(x, y, z)$, is a noisy ultrasound volumetric image, $g(x, y, z)$ is the noise-free ultrasound volumetric image, $\eta(x, y, z)$ and $\beta(x, y, z)$ are the multiplicative and additive noise respectively. The additive noise $\beta(x, y, z)$ is assumed to follow a Gaussian distribution with variance $\sigma(x, y, z)$ and an expected value $E(\beta(x, y, z)) = 0$ in all directions. In this framework, the expected value of the difference between the measured volumetric image and the contribution from the multiplicative noise is equal to the expected value of the additive noise and is assumed to be equal to zero:

$$E(f(x, y, z) - g(x, y, z) \times \eta(x, y, z)) = E(\beta(x, y, z)) = 0 \quad (3.2)$$

Therefore, it seems logical to transform the original measured ultrasound images with a logarithmic function, where the multiplicative speckle noise becomes additive:

$$\log[f(x, y, z)] = \log[g(x, y, z)] + \log[\eta(x, y, z)] \quad (3.3)$$

In order to respect this condition, one must first filter $f(x, y, z)$ using Anisotropic Geodesic (AG) Filter capable of preserving key features and reducing the effect of additive noise and then perform a logarithm transform of the resulting image to convert the multiplicative noise to additive noise as demonstrated in equation (3.3), then filtered again with a similar filter (AG) to eliminate the noise. An inverse log-function is then applied to the image produced by this second filter. The purpose of the inverse log-function is just to remove the logarithm operation effect. These process steps illustrate in Figure 3.1 that show the block diagram of the proposed filtering approach.

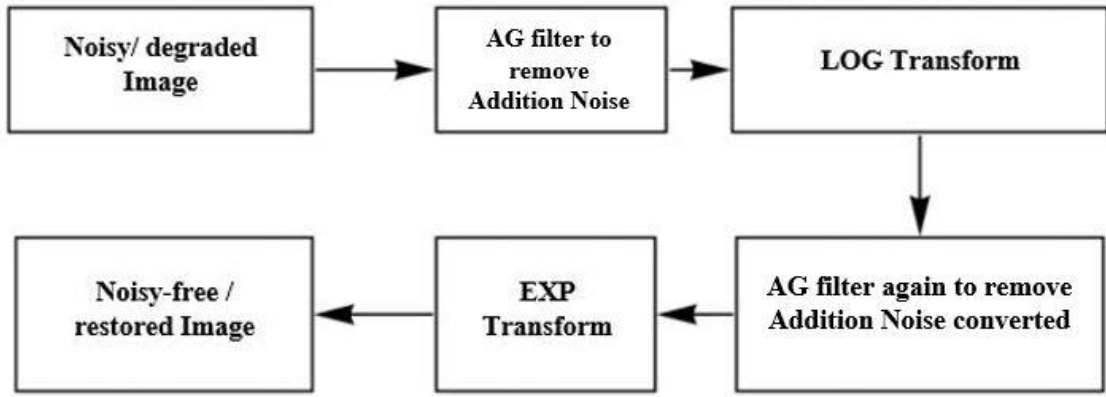


Fig. 0.2: Block diagram of the proposed filtering approach

3.3 Geodesic Filter Algorithm

The proposed algorithm is similar to Gaussian filtering but can adapt to local intensity and geometry variations. Similar to standard Gaussian filtering, the filter can produce a multi-resolution scale-space representation with very interesting properties such as edge or boundary preservation. Let us now discuss in more details the geodesic filter.

A sample collection of 3-D measurements corresponding to an area observed in a specific sensor point was used in the original definition range images, Piotr Osinski, Jakub Markiewicz, Jarosław Nowisz, Michał Remiszewski, Albert Rasiński and Robert Sitnik. (2022).

The filter can be applied to any complex signal, including color range pictures, MRI, and CT scans. One of the algorithm's most essential qualities is its ability to filter continuous regions while maintaining the localisation of critical features.

This is an important characteristic for medical applications. In continuous regions, the filter behaves like a Gaussian filter, whereas in regions with abrupt discontinuities, it behaves like an anisotropic filter. Its greater capability at filtering ultrasonic pictures was demonstrated in experimental comparisons with two of the most well-known filters.

To explain this filter in detail, we will first explain the definition of geodesic distance or geodesic trajectories and then present how to compute the geodesic distance using a single source shortest path algorithm that was developed for the purpose of this work.

3.3.1 Geodesic Distances

The actual length of the minimum path defined on the 4D manifold is an interesting geodesic metric. In the manufacturing multiple, the generalized geodesic distance $d_s = (p, q)$ between two points p and q is defined as the shortest length L_s of all the paths linked to q . These geodesics trajectories maybe called minimal paths since the sum of the grey-levels

and the spatial distance along these paths is minimum. Let us now discuss how to compute these geodesic trajectories and distances.

3.3.2 Geodesics Trajectory algorithm using Single-Source Shortest Path Algorithm

In order to achieve geodesic distances from a convolution window's center point to its neighboring points, a minimum trajectory must be found between the center and all other points on the window. From Piotr Osinski, Jakub Markiewicz, Jarosław Nowisz, Michał Remiszewski, Albert Rasiński and Robert Sitnik. (2022), we know that the manifold distances d_s and that is the minimum distance between the two points $p(u, v)$ and $q(u-\tau, v-\zeta)$ between all trajectories $p(u_i, v_i)$ and $q(u_{i+1}, v_i)$ are described:

$$d_s(p, q) = \min_{\alpha} s_{\alpha}(p, q) \quad (3.4)$$

Where $s_{\alpha}(p, q)$ is the cumulative arc-length between the two points for a trajectory α joining them on the manifold? Note that the value of d_s will be large if the minimum trajectory goes across for example an intensity discontinuity. From the above equation, one can design an efficient algorithm to compute the geodesic distances by using the Single-Source Shortest Paths Algorithm for weighted graphs, Nikpour, M., & Hassanpour, H. (2010).

The diagram vertices are the points in the convolution window and the edges are the next-door connections. The discrete arc of the edges between points, for example. $p(u_i, v_i)$ and $q(u_{i+1}, v_i)$ is given by:

$$\sqrt{||d(u_i, v_j) - d(u_{i+1}, v_j)||^2} \quad (3.5)$$

3.4 Ultrasound Medical Imaging Restoration

In this study, we were able to demonstrate that by adapting a non-linear filter developed to process range images, we were able to filter multiplicative noise in ultrasound images. This filter called anisotropic geodesic filter possess similar quality as the well-known anisotropic gradient-based filter from Perona P., Malik J. (1990) but do not require to compute image gradients and is free of non-intuitive parameters like integration time and diffusion coefficient. The filter can be easily generalized to any complex signals such as colour range images, MRI, CT etc. One of the key properties of this algorithm is its ability to filter continuous regions without the loss of localization of important features. This is a key property for medical applications. The filter is akin to a Gaussian filter in continuous regions and responds like an anisotropic filter in regions

with sharp discontinuities. Experimental comparisons with two of the most well-known filters were able to demonstrate its superior capability at filtering ultrasound images.

This filter has numerous potential applications in medical imaging and image processing. Its applications are not just limited to medical and medicine field but can also be used to suppress speckle noise from SAR images as well. In case of ultrasound, it can be used to improve surgical guidance and robotic-assisted interventions which necessitate high quality images where the filtering can be embedded directly in the ultrasound machine.

The algorithm to find the minimum distances, Grecksfor Grecks (2021), is given as follows:

Input: $G = (V,E)$ (a weighted graph) and v (the source vertex corresponding to the center point)

Output: for each vertex w , $w.sp$ is the length of the shortest path from v to w and corresponding minimum trajectories w,tr

```

begin
for all vertices  $w$  do
  /* $w.mark$  indicates if the vertex distance is determined*/
   $w.mark := false;$ 
   $w.sp := \infty;$ 
 $v.sp = 0;$ 
 $v.tr = 0;$ 
while there exists an unmarked vertex do
let  $w$  be an unmarked vertex such that  $w.sp$  is minimum;
 $w.mark := true;$ 
for all neighboring edges  $(w,x)$  such that  $x$  is unmarked do
if  $w.sp + length(w,x) < x.sp$  then
 $x.sp := w.sp + length(w,x);$ 
 $x.tr := w;$ 
end

```

In this algorithm the distances between a number of track lengths must be determined and track lengths must be periodically updated. We use a heap structure to execute this efficiently. The existing established shortest track length from center point V are held in a heap with all undeclared vertices. To find an undeclared vertex so we can only take it from the top of the heap to make the trajectory $w.sp$ a minimum. We can monitor all the edges linked to the vertex and easily upgrade path lengths.

3.5 Filtering a 3D and 2D Ultrasound Images

For a 3D ultrasound represented by a voxel space $V(i, j, m)$ each slice located at position z_m is represented by a 4D manifold $r_m(i, j) = (x_m(i, j), y_m(i, j), z_m(i, j), \ln V(i, j, m))$. Equation 3.8 is reduced for each slice z_m to:

$$\hat{v}(i, j, m) = \exp\left(\frac{\sum_{k=-W/2}^{k=W/2} \sum_{l=-W/2}^{l=W/2} \ln(V(i+k, i+l, m)) \exp(-d^2(r_m(i+k, j+l), r_m(i, j))/(2\sigma^2))}{\sum_{k=-W/2}^{k=W/2} \sum_{l=-W/2}^{l=W/2} \exp(-d^2(r_m(i+k, j+l), r_m(i, j))/(2\sigma^2))}\right) \quad (3.6)$$

where the logarithmic transformation for the multiplicative noise case is included. For the 2D case, Equation 3.5 is simply when $m = 1$

In this chapter, a filtering method to reduce speckle noise, based on geodesic calculation for two-dimensional and three-dimensional cardiac ultrasound is proposed. In the next chapter, we will demonstrate that the proposed filter can reduce speckle noise better than the two filters mentioned in literature review. We will demonstrate that it is a good choice to filter curves and edges in an ultrasound image as it preserves these features localization automatically. In the writing, the writers have considered ultrasound pictures (normal/manufactured) with falsely added dot commotion content and have proposed techniques for smothering this spot clamor in such pictures. Be that as it may, in this proposal, we use pictures estimated by genuine ultrasound gear which contain inborn spot commotion.

CHAPTER FOUR

EXPERIMENTS

In order to demonstrate the performance of the intrinsic filter, we performed a systematic comparison with the most two well-known filters found in the literature: Gaussian filter, median filter. This comparison was achieved by measuring traditional distortion measures such as contrast-to-noise-ratio (CNR), signal to-noise-ratio (SNR), mean-square error (MSE), peak signal-to-noise-ratio (PSNR), and correlation coefficients between reference images.

4.1 Image Data Set

For the purpose of this comparison, echocardiography scans from a cardiac ultrasound phantom with known dimension as well as six human volunteers were acquired using the Siemens ACUSON SC2000 ultrasound scanner. It was taken from a patient named examined by the Dr. Saad, Zidan, Baqubah hospital, Diyala city (2021). The first data set had a 50 2D images of 558 x 558 pixels with an image size of (79.5 KB) and the second data set was measured from six patients which included parasternal and apical views of their heart. The number of volume data frames were 7 - 34 per cardiac cycle with a volumes size of 137 x 131 x 120 voxels with a voxel size of (0.74 mm x 0.74 mm x 0.63 mm). To reduce the presence of additive noise each volume slices were first filtered by a Gaussian filter of size 5×5 with $\sigma = 0.5$.

4.2 2D Ultrasound Filtering Results

Let us look first visually at the evolution of a slice in both data sets as a function of each filter parameters. One can see at Figure 4.1 and 4.2 the evolution of the ultrasound slice images as a function of the parameter σ for the Gaussian filter and at Figure 4.3 and 4.4 the evolution of the same ultrasound slice images with median filters with window sizes from 3×3 , 5×5 , and 7×7 . As expected, the Gaussian filter can reduce the speckle but at the expense of losing important features. On the other hand, the median filter is capable of filtering the speckle without the loss of small feature when the window size is small but as the window increase the median filter loses fine image features like Gaussian filter. In Figure 4.5 and one can see the result of the proposed geodesic filter. One can see that not only does the proposed filter reduce speckle noise as a function of σ but also preserves boundaries and fine features.

Noisy Image at sigma = 1 (L) G F Image (R)

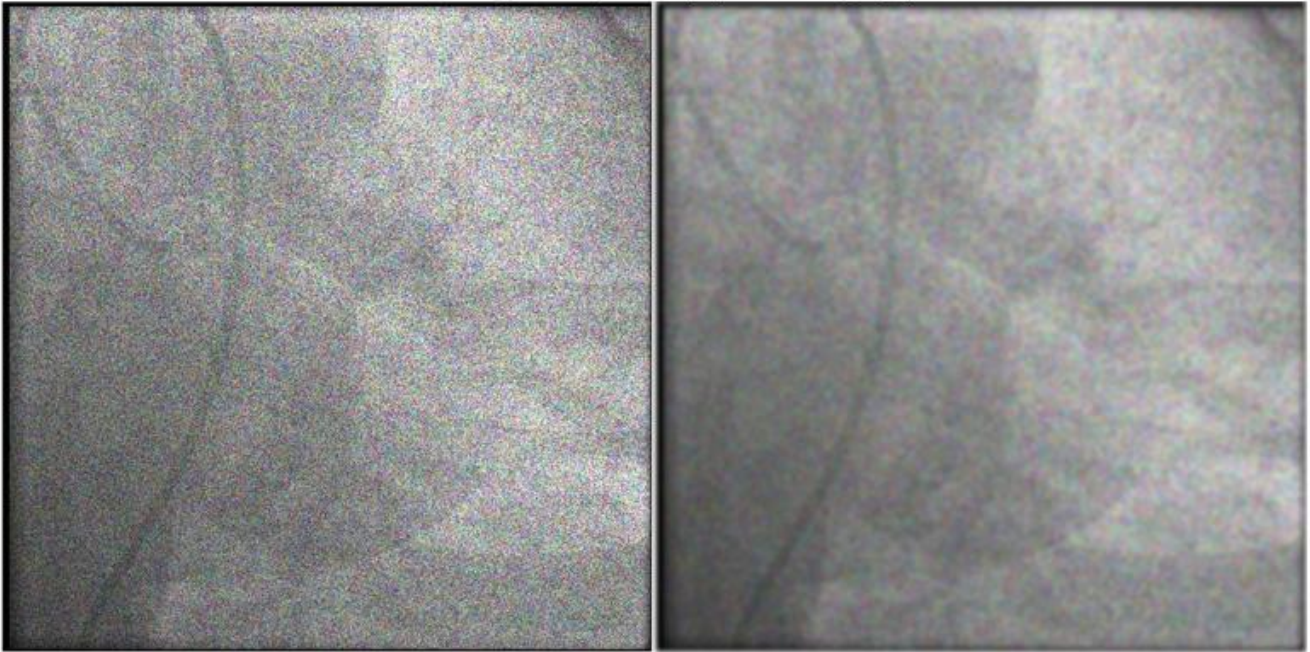


Fig. 0.1: Gaussian filter $S=1$



Noisy Image at sigma = 1.5 (L) G F Image (R)

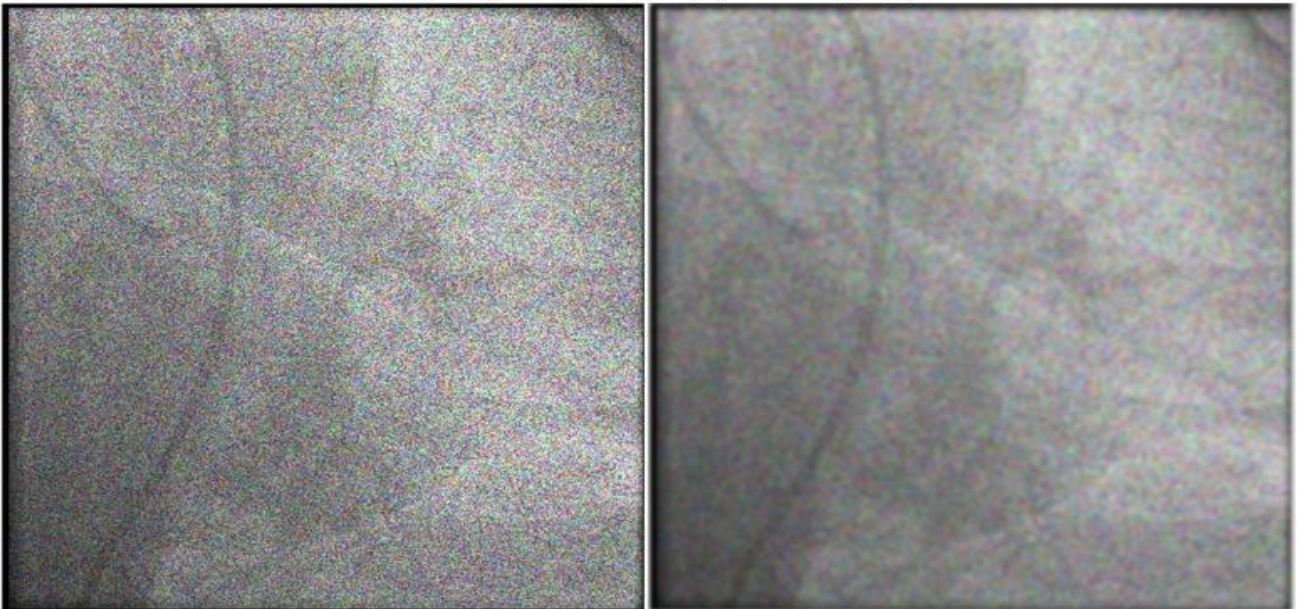


Fig. 4.2: Gaussian filter $S=1.5$

Noisy Image at sigma = 2 (L) G F Image (R)

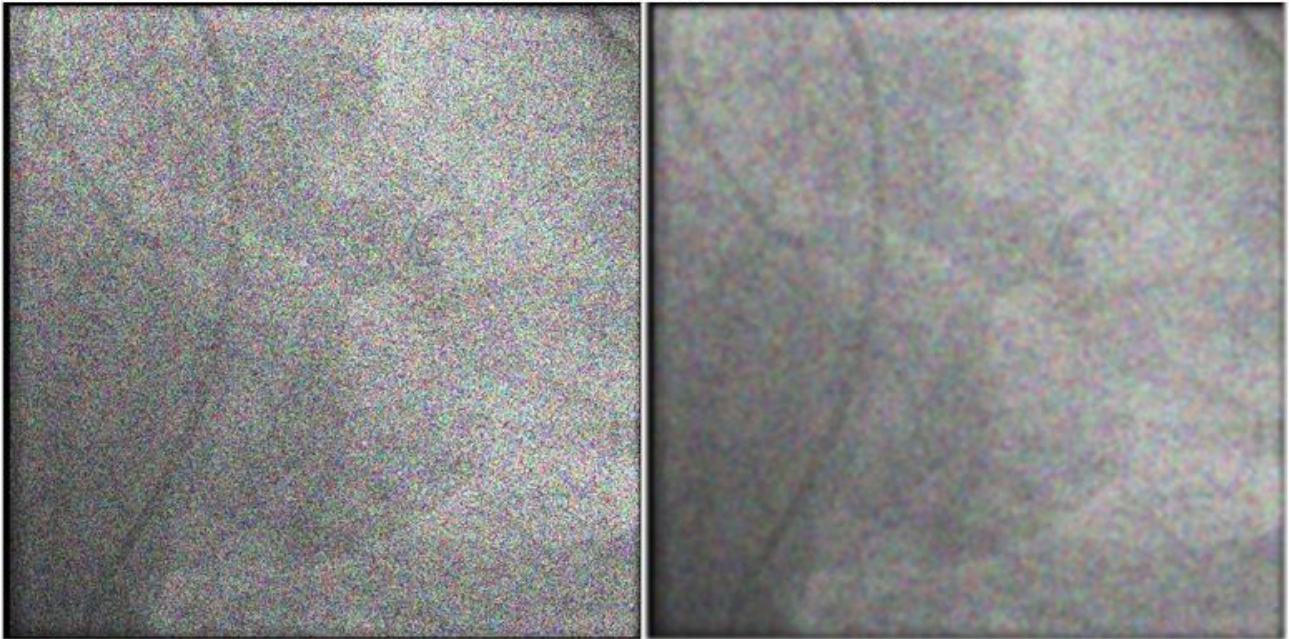
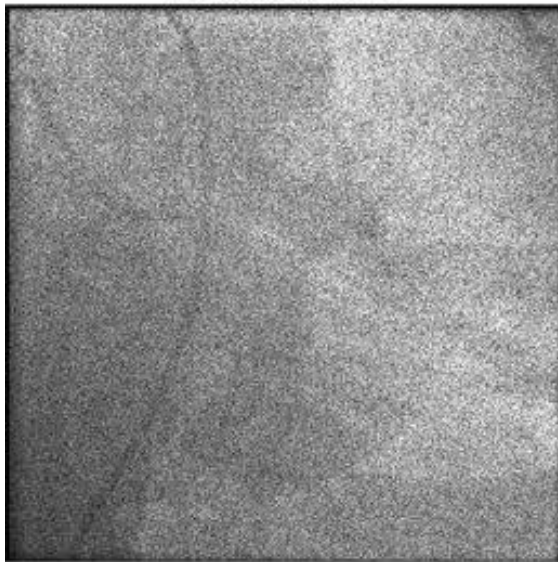


Fig. 0.2: Gaussian filter S=2

noisy Image S=1



output of median filter

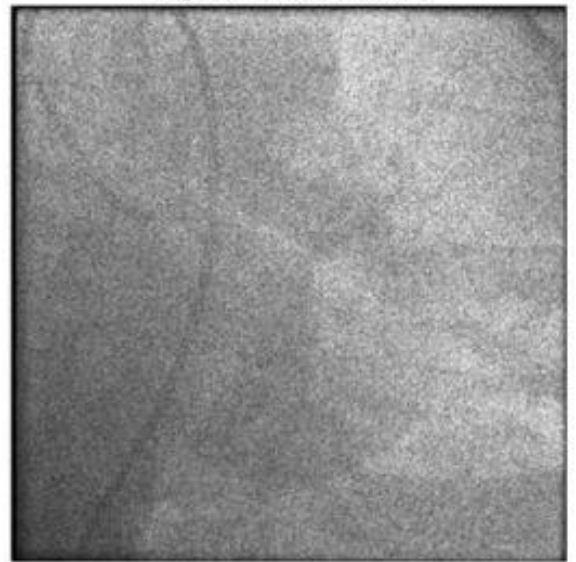
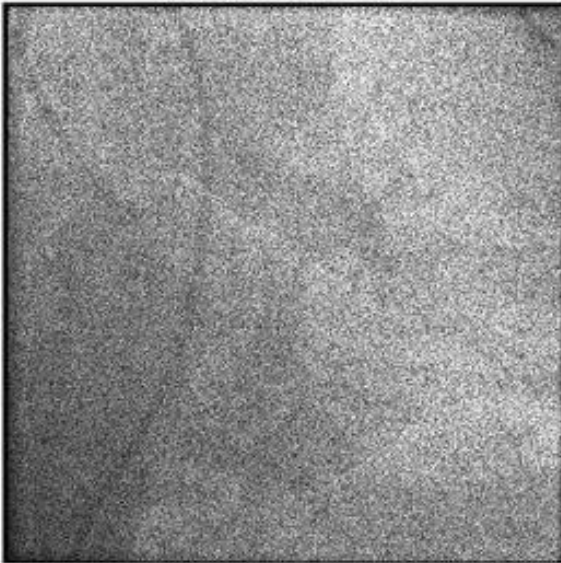


Fig. 4.4: Median filter S =1

noisy Image S=1.5



output of median filter

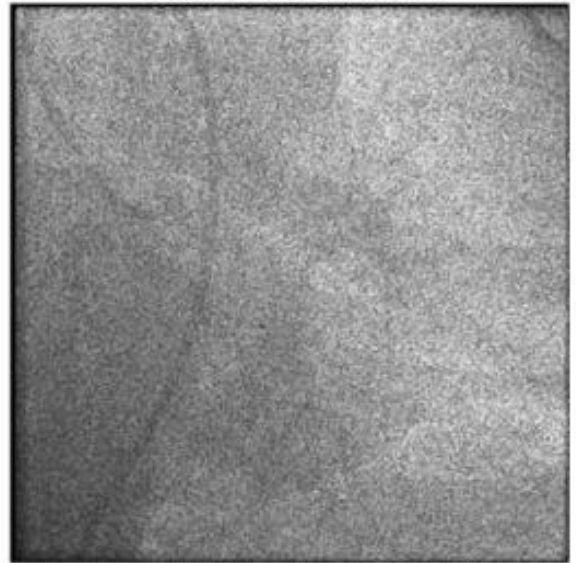
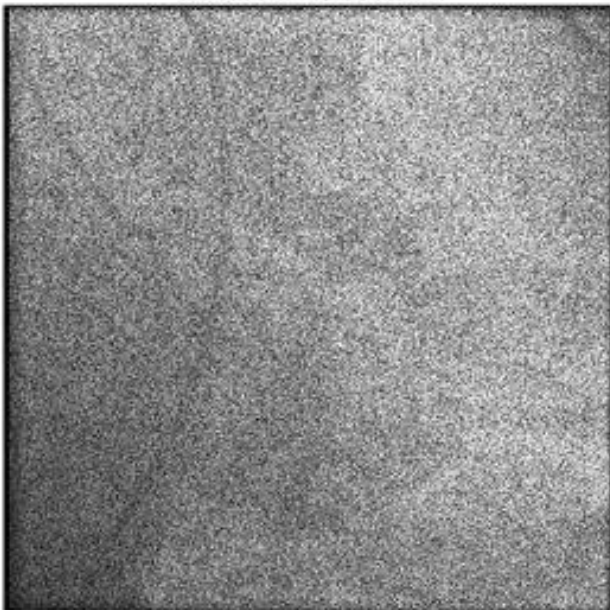


Fig. 0.3: Median filter at S=1.5

noisy Image S=2



output of median filter

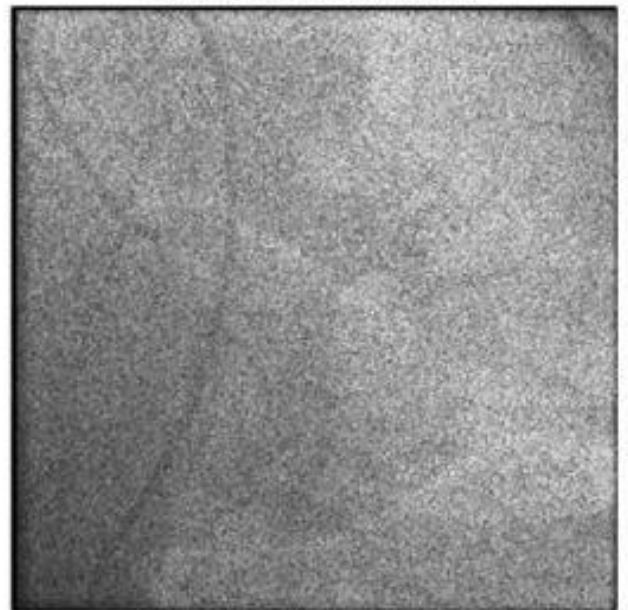
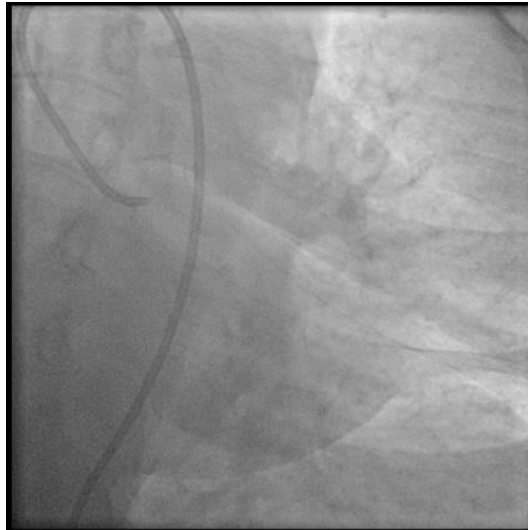
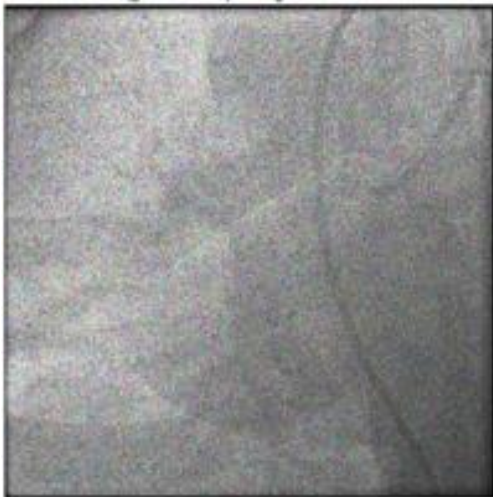


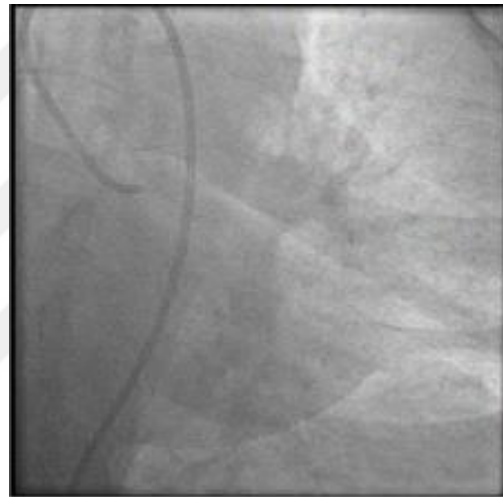
Fig. 0.6: Median filter at S=2



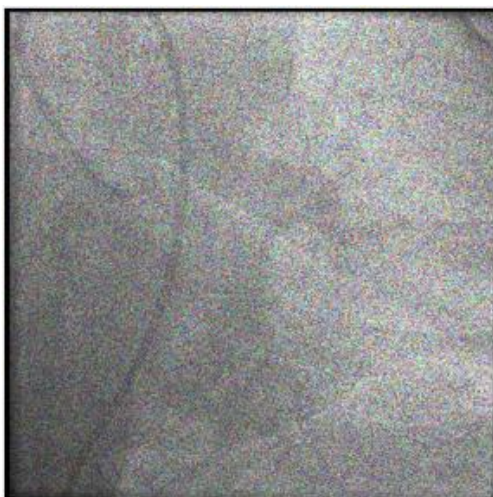
a. Original Image



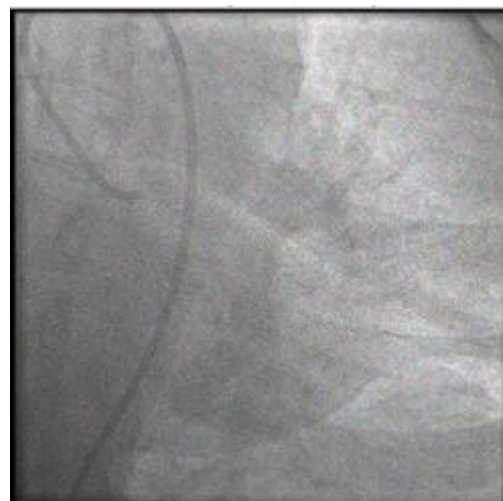
b. At Sigma = 1



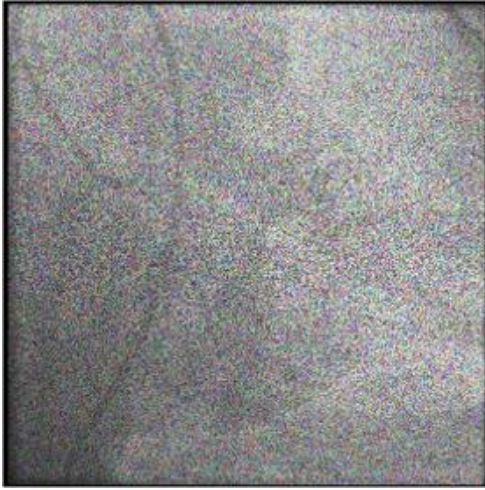
c. After AG filter



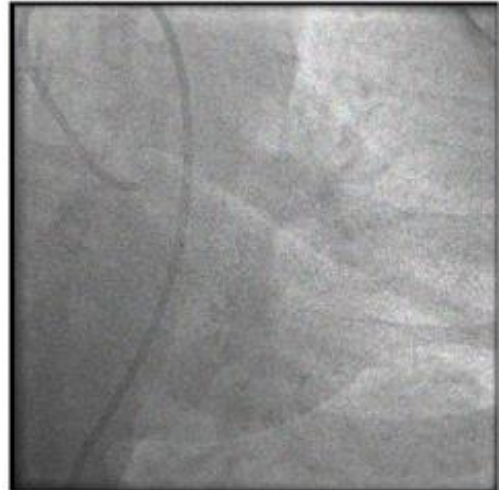
d. At sigma = 1.5



e. After AG filter

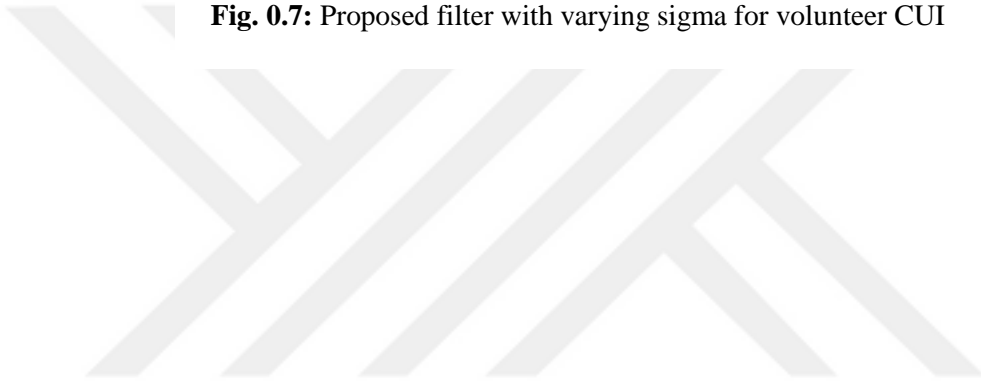


f. At sigma = 2



g. After AG filter

Fig. 0.7: Proposed filter with varying sigma for volunteer CUI



4.3 3D Ultrasound Filtering Results

Before systematically comparing the results with the other filters, we would like to show for the different data sets results for the geodesic filter only. The 2D implementation of the geodesic anisotropic diffusion is extended to 3D as described in Chapter 3. The implementation of the filter was done in MATLAB and the vis3D function was used to display the 3D data set. One can see in the Figure 4.8 the original cardiac phantom data set in the YX-plane, YZ-plane, and XZ-plane as well as a combined 3D rendering. One can see in Figure 4.9 the filtered volume for $\sigma = 5$. One can see in the Figure 4.10 the original cardiac patient data. One can see in Figure 4.12 the filtered volume for $\sigma = 5$. While Figures 4.11, 4.12, 4.13, 4.14 and 4.15 demonstrate the anisotropic filter at 3D for $\sigma = 5$, at 3×3 window size, 5×5 window size, 7×7 window size and 11×11 window size, respectively.

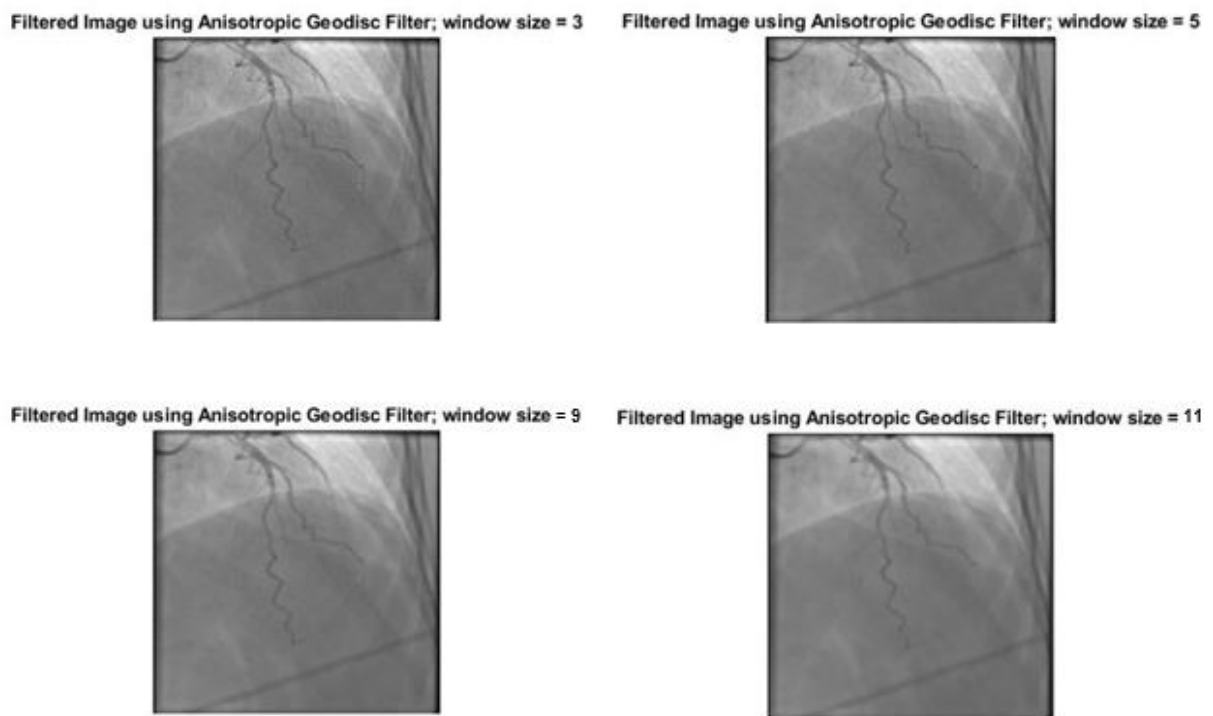


Fig. 0.8 Proposed filter with varying window size for volunteer CUI

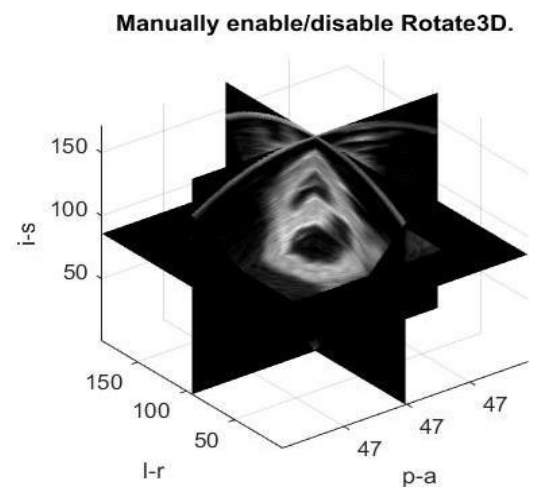
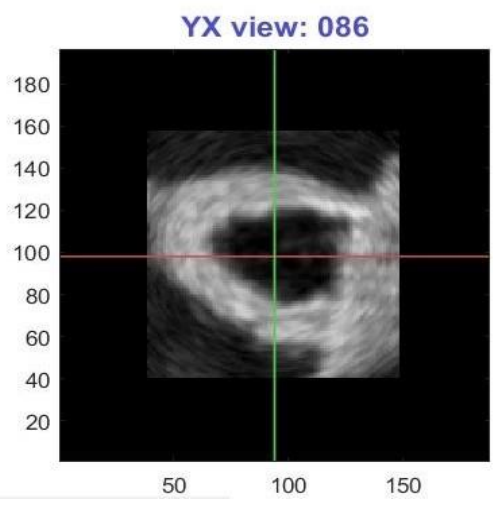
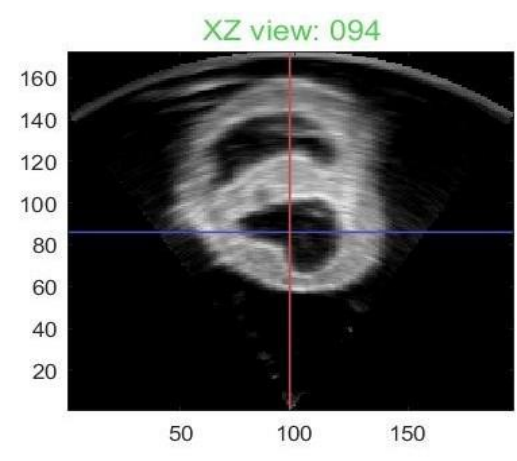
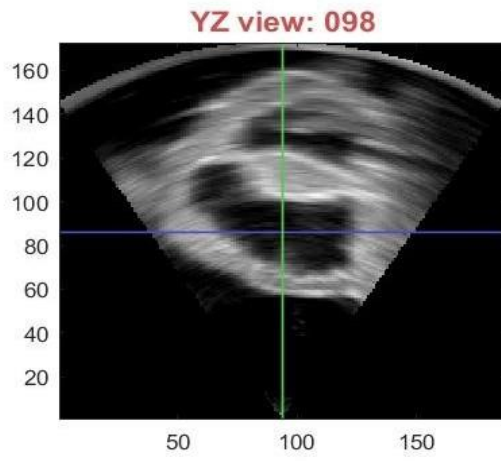


Figure 0.9: Original cardiac phantom ultrasound.

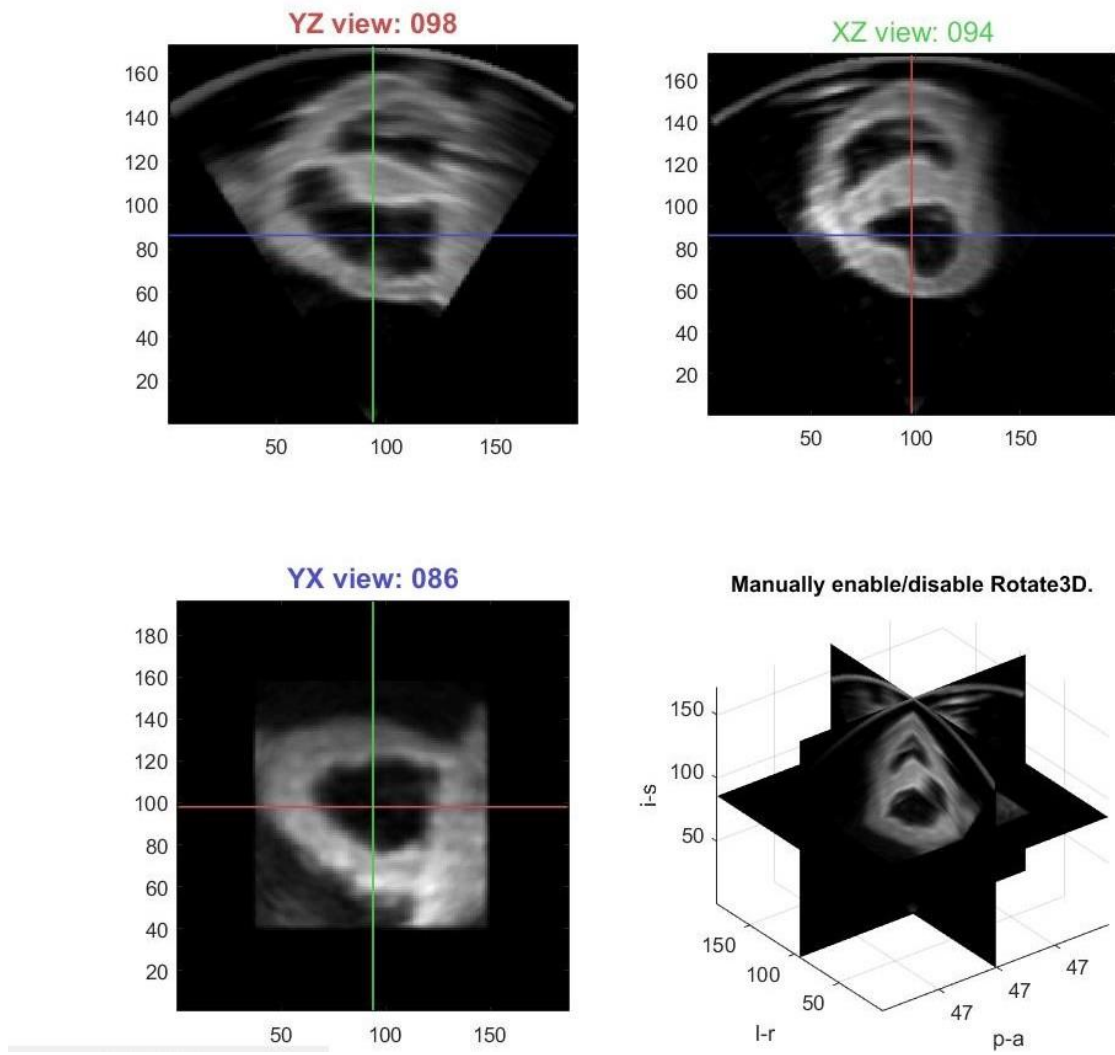


Fig. 0.10: Proposed 3D filter for the cardiac phantom ultrasound $\sigma = 5$

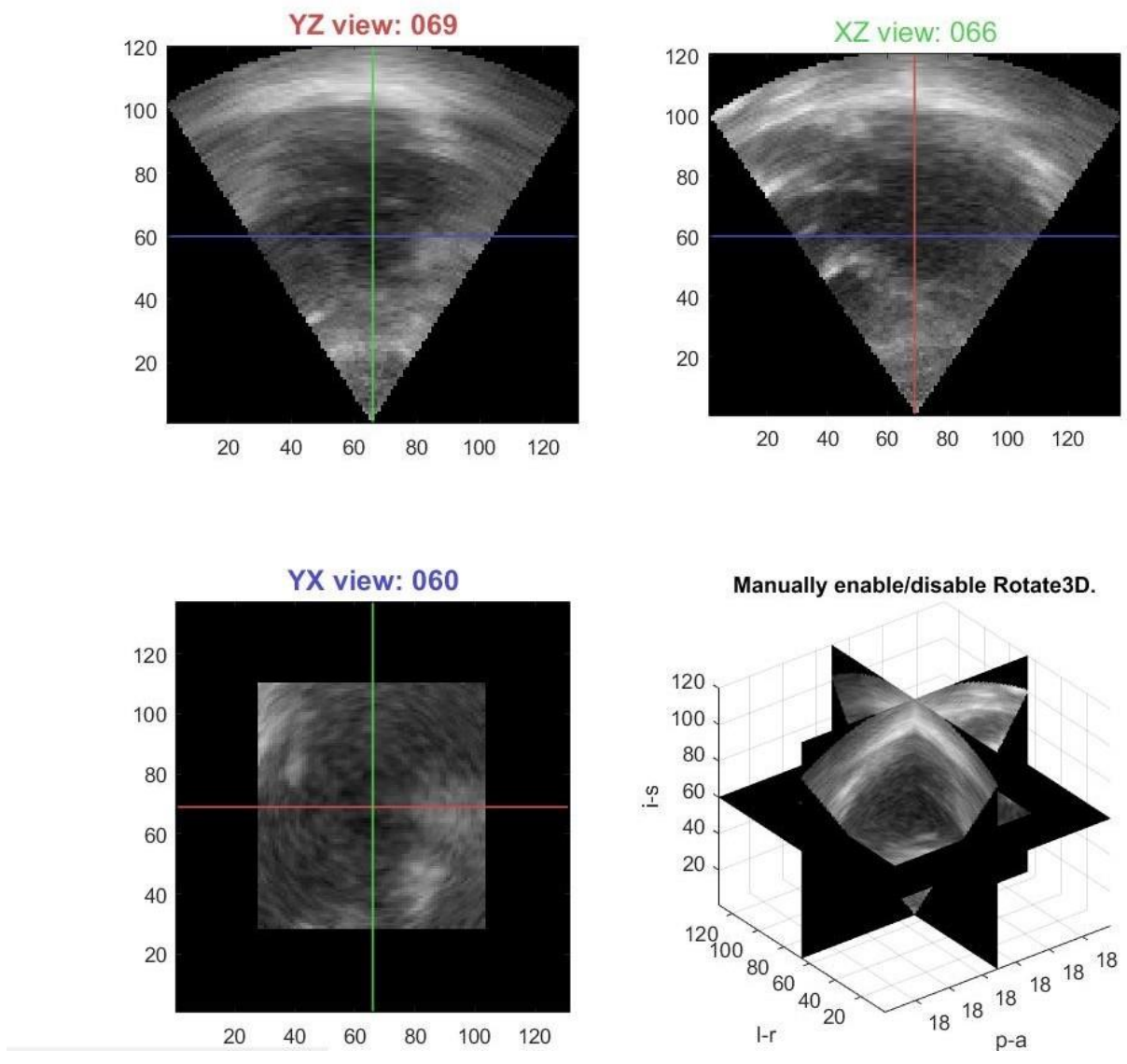


Fig. 0.11: Original volunteer cardiac ultrasound

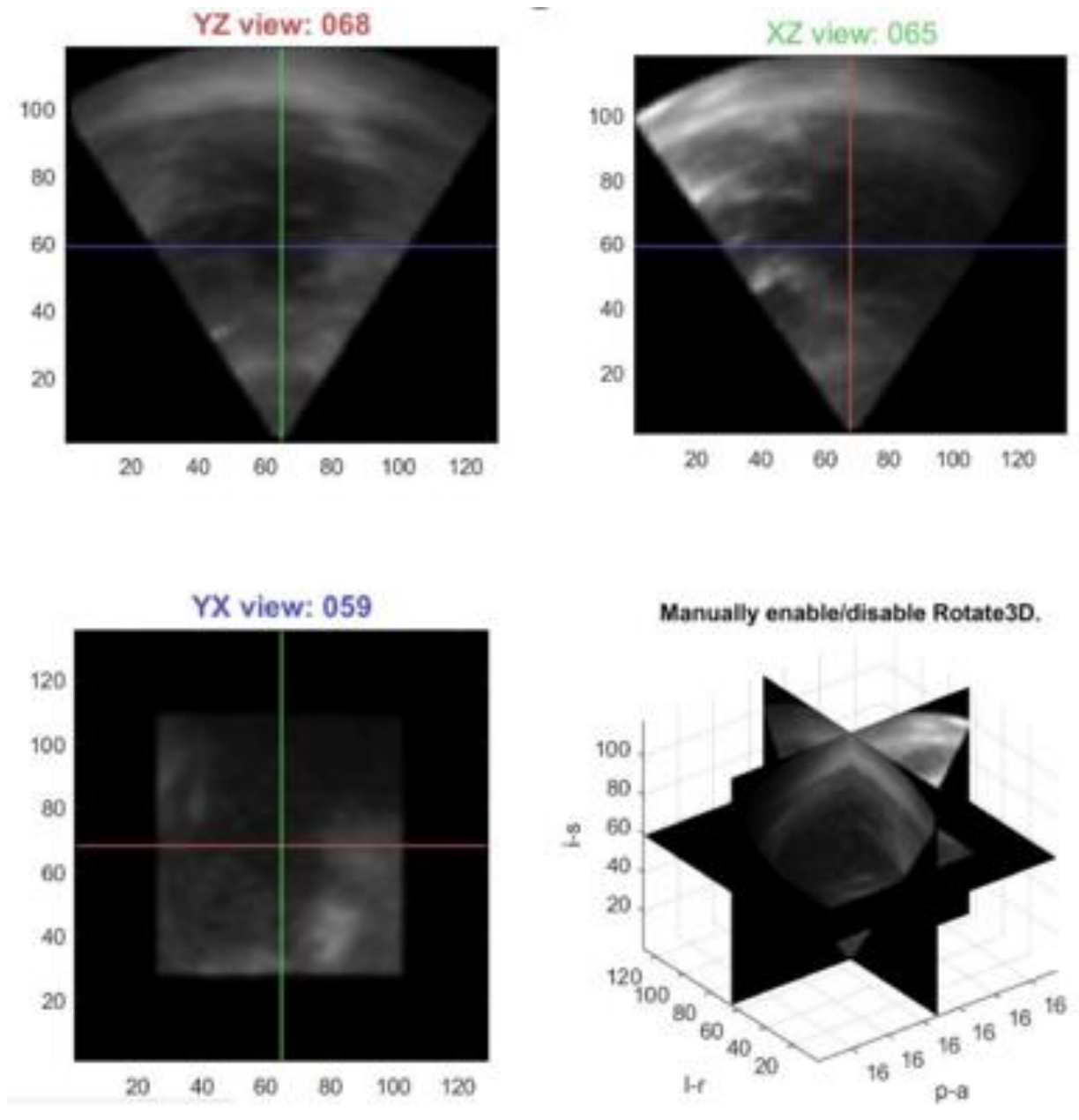


Fig. 0.42: Proposed 3D filter for Volunteer cardiac ultrasound for $\sigma = 5$

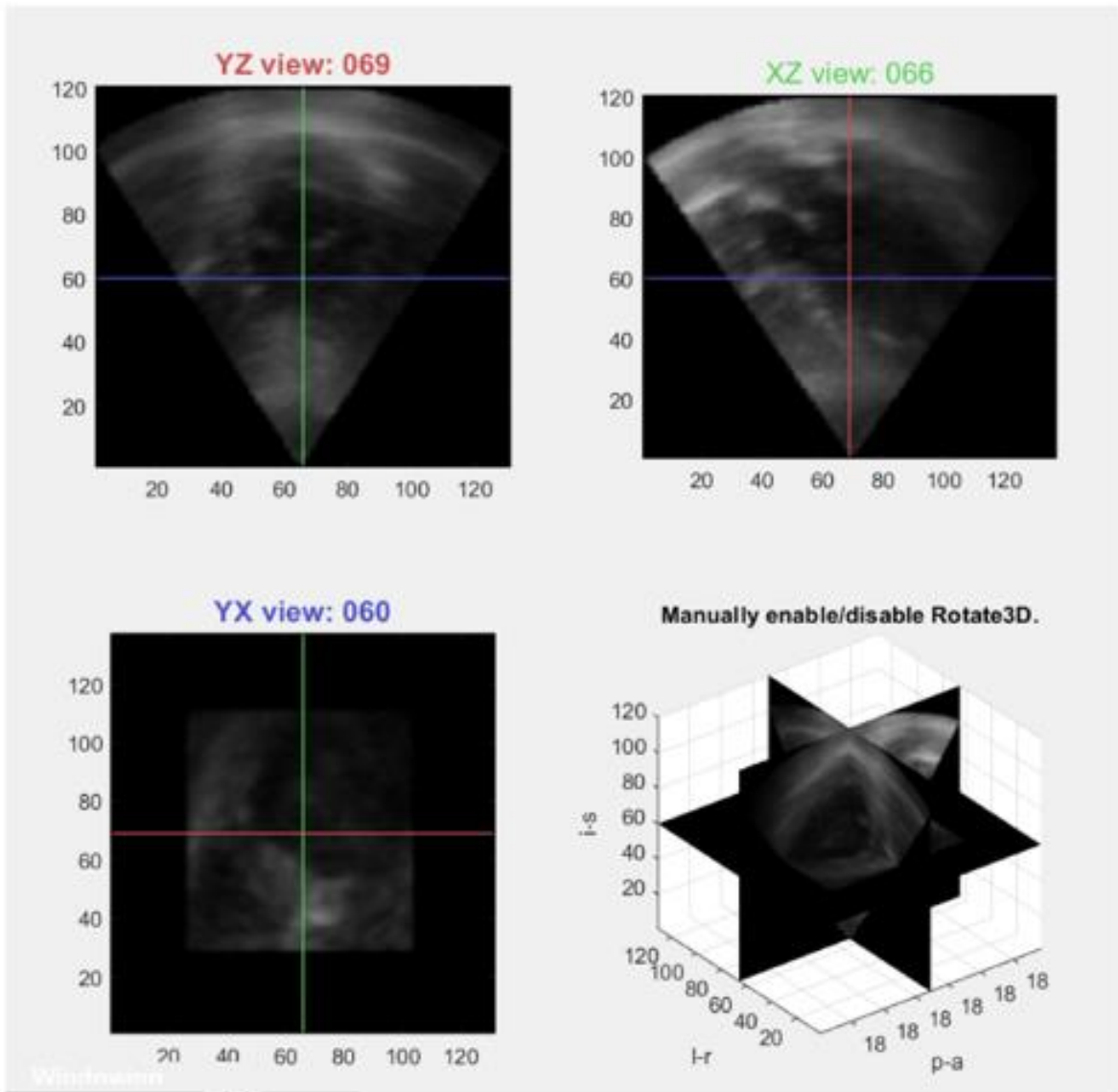


Fig. 0.13: Proposed 3D filter for volunteer cardiac ultrasound for windows size=3x3

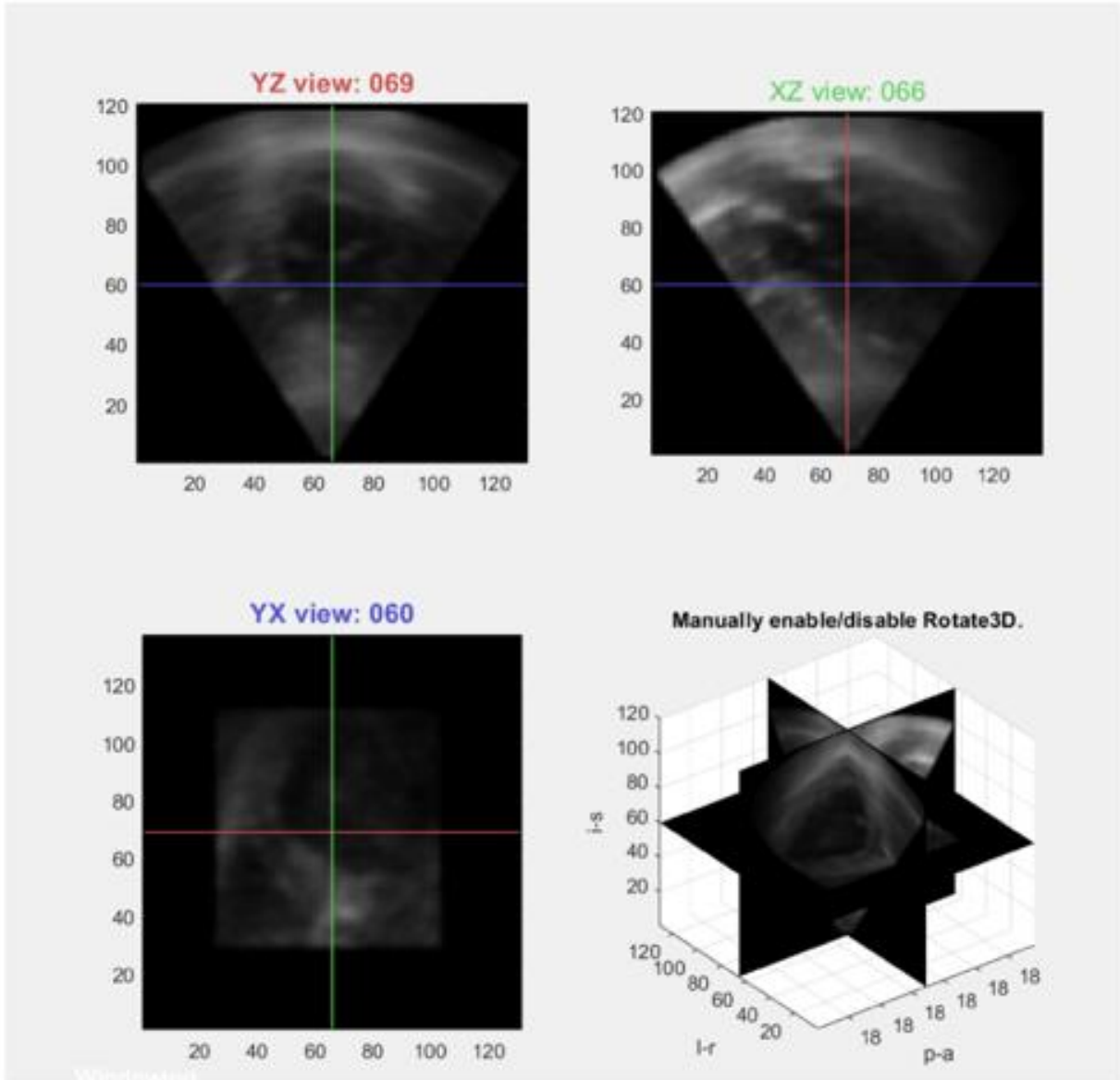


Fig. 0.54: Proposed 3D filter for volunteer cardiac ultrasound for windows size=5x5

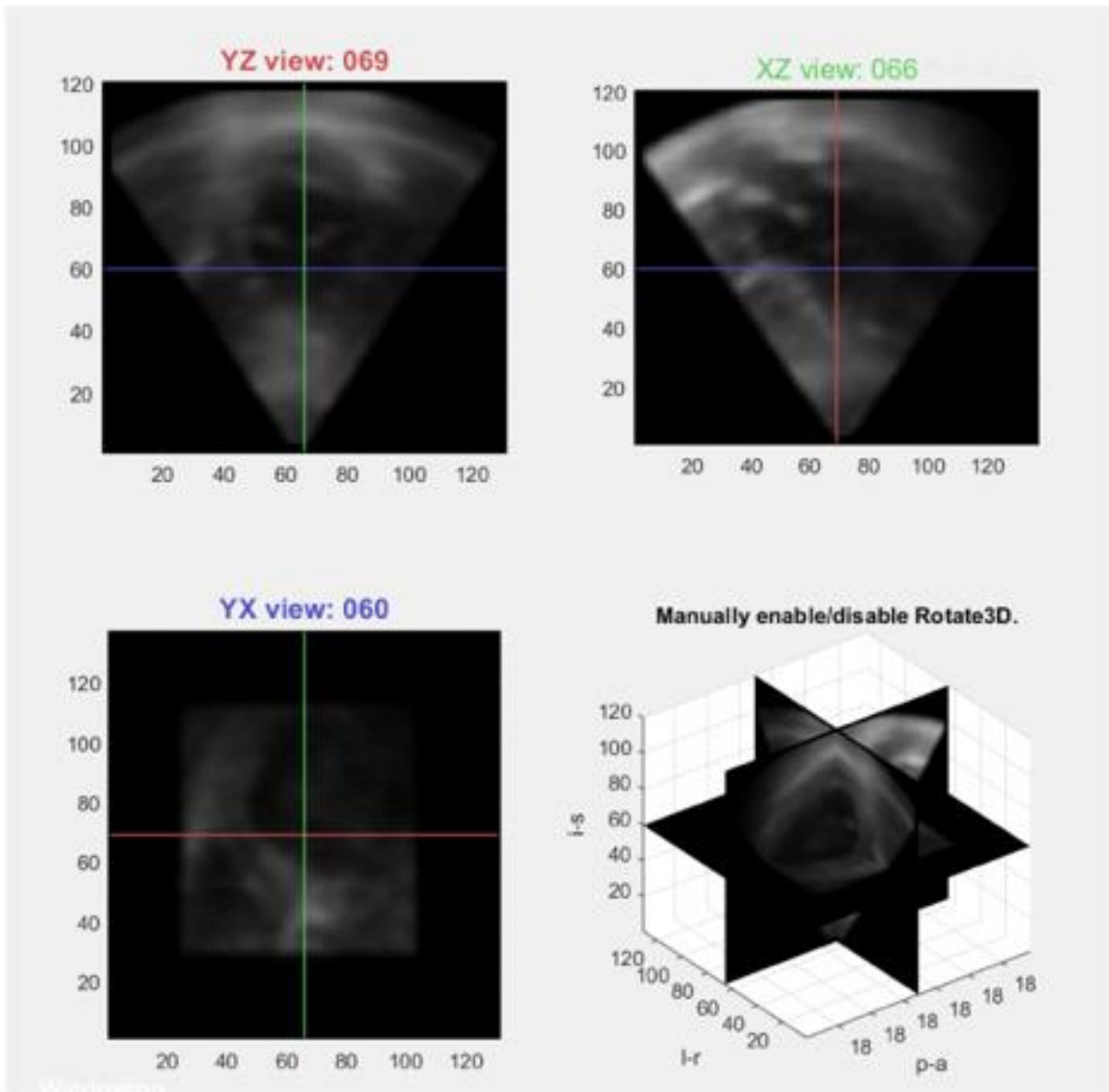


Fig. 0.15: Proposed 3D filter for volunteer cardiac ultrasound for windows size=7x7

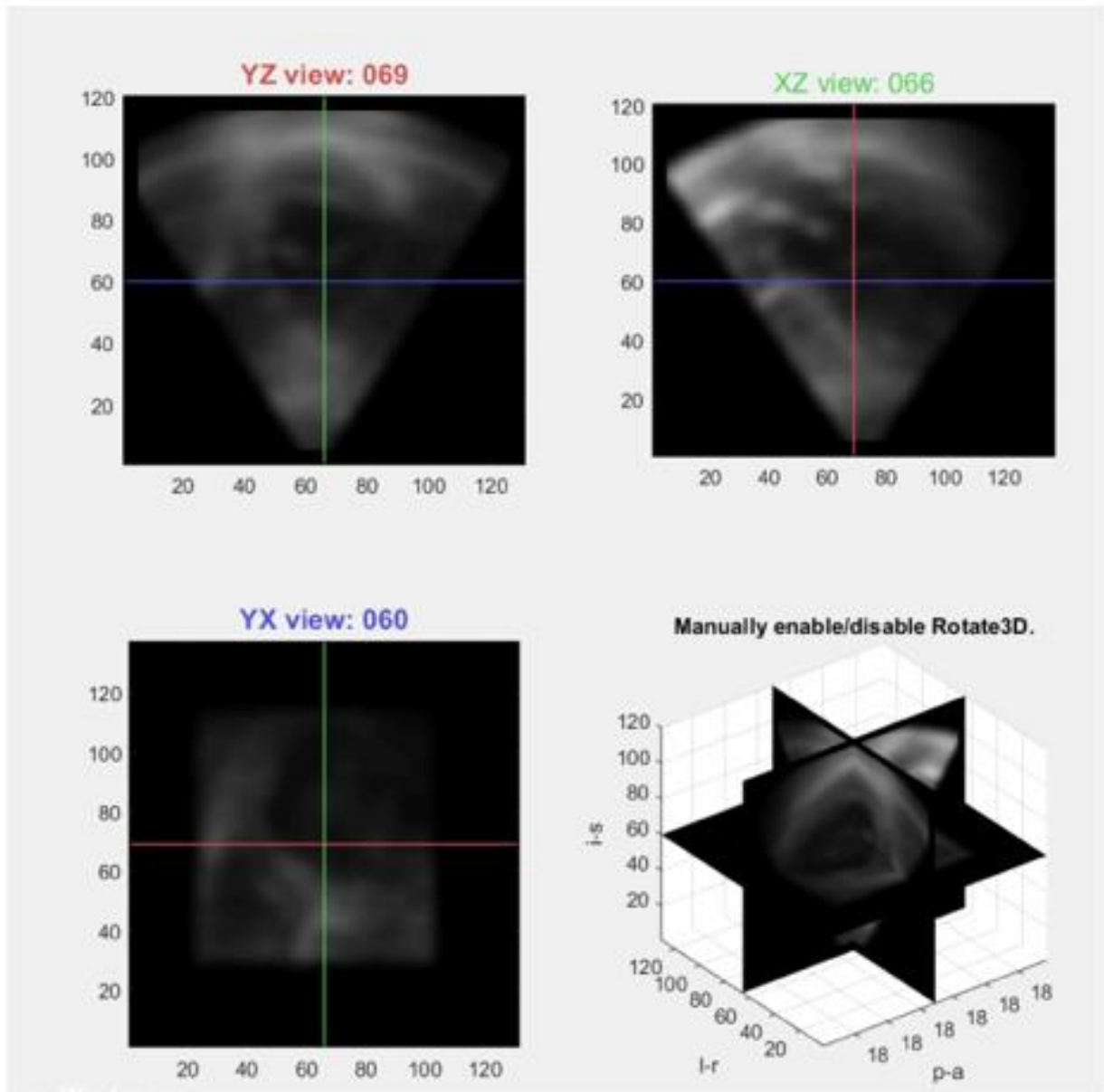


Fig. 0.16: Proposed 3D filter for volunteer cardiac ultrasound for windows size=11x11

For visual comparison, one can see in Figure 4.17, 4.18 and 4.19 the filtering results for the two other methods.

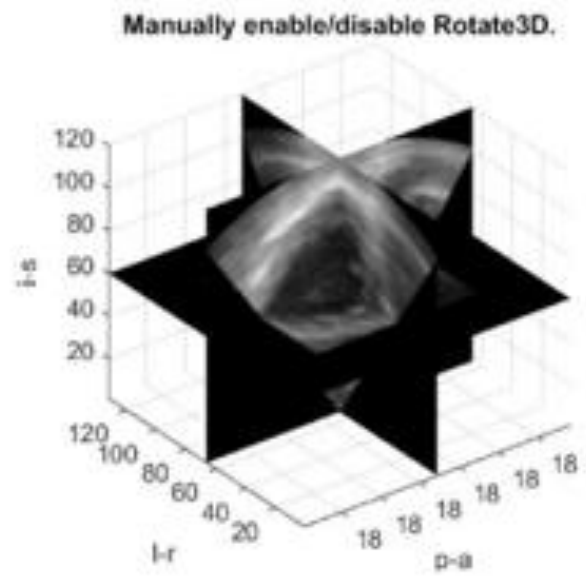
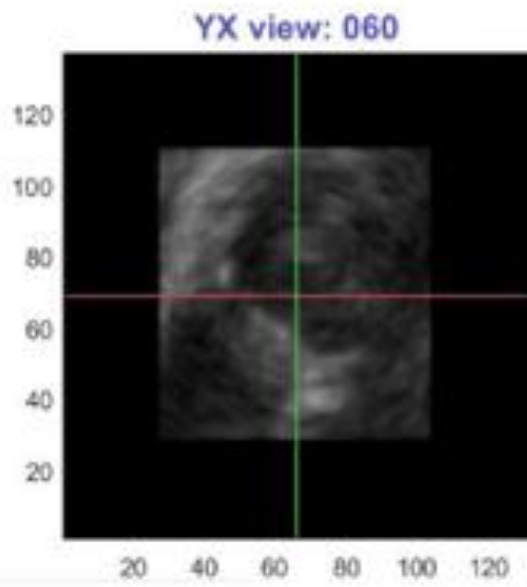
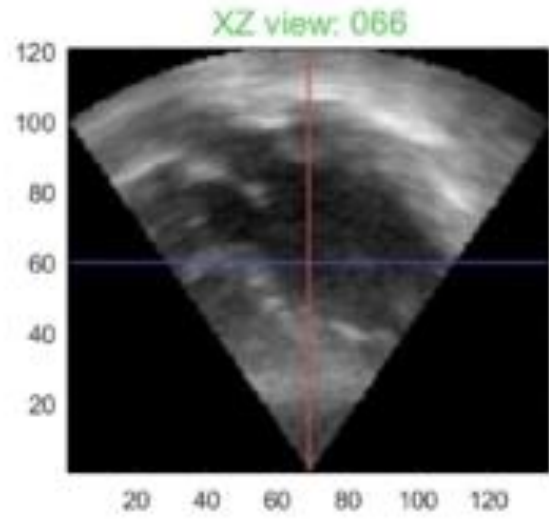
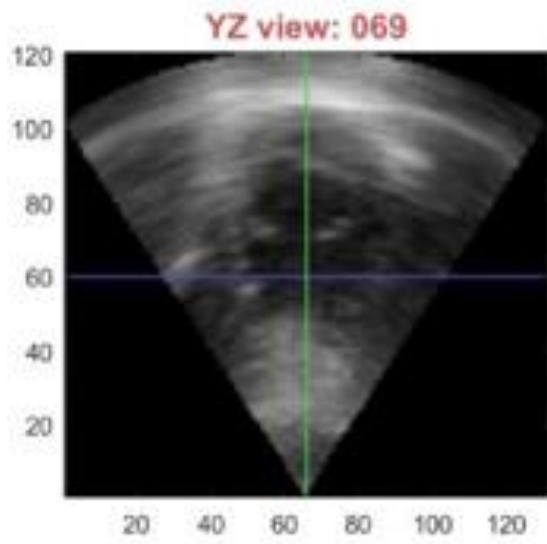


Fig. 0.17: Gaussian Filter-Volunteer CUI for $\sigma = 5$

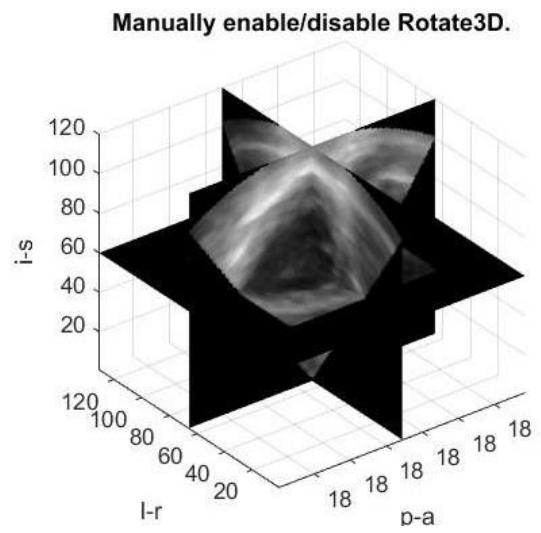
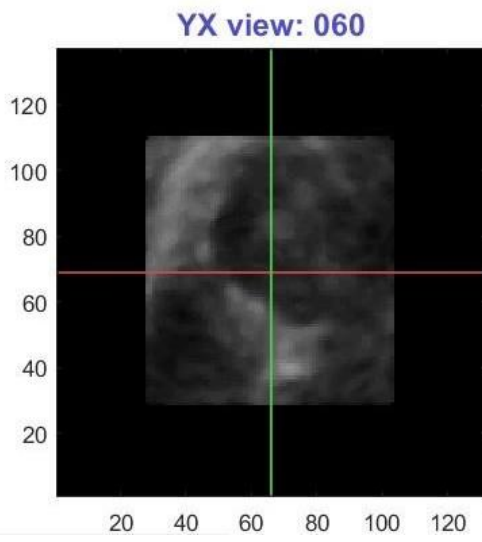
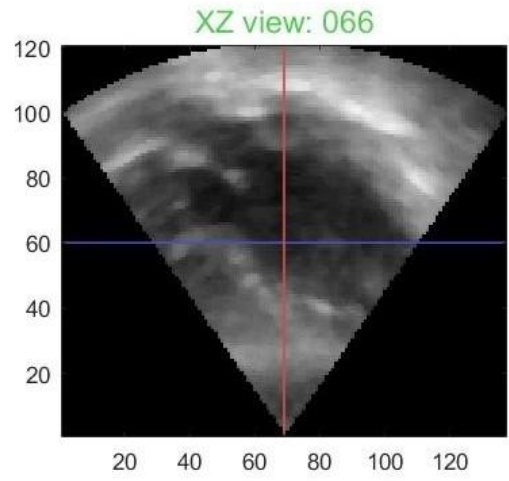
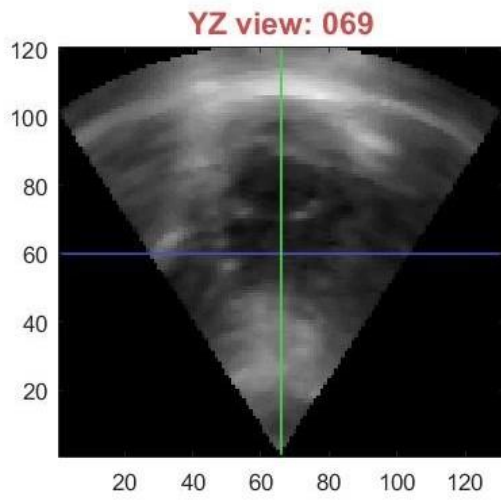


Fig. 0.18: Median filter - volunteer CUI for a window size of 5×5

4.4 Quantitative Analysis

This section describes a number of quantitative validation measures used to assess the quality of ultrasound images filtering using well known metrics such as: image contrast (IC), CNR, SNR, and PSNR. Let's first define those metrics mathematically and then study how the four filters compare to each other.

4.4.1 Signal-to-Noise-Ratio

The ratio between average and standard pixels variance values within a range of interests is defined as SNR for a quantitative comparison, i.e., the percentage of change in the SNR, i.e., the SNR for filtering:

$$\Delta SNR = \frac{\Delta(SNR)^{my} + \Delta(SNR)^{bp}}{2}, \quad (4.1)$$

where $\Delta(SNR)^{my}$ and $\Delta(SNR)^{bp}$ denote the percentage of change in the SNR in the myocardial and blood-pool regions, respectively. The percentage of change in SNR in the myocardial region, $\Delta(SNR)^{my}$, is computed as:

$$\Delta(SNR)^{my} = \left[\frac{\frac{\mu_f^{my}}{\sigma_f^{my}}}{\frac{1}{N} \sum_{i=1}^N \left(\frac{\mu_i^{my}}{\sigma_i^{my}} \right)} - 1 \right] * 100, \quad (4.2)$$

The percentage of change in SNR in the blood-pool region, $\Delta(SNR)^{bp}$, is computed in a similar way to $\Delta(SNR)^{my}$. SNR is a strong spring strength test. The higher the SNR, the lower the sprinkling noise and the greater the sprinkling effect. When SNR is measured it is taken as the average between the myocardial and blood-pool regions.

4.4.2 Root-Mean-Square-Error

The MSE helps us to compare our original image with our decayed picture version for "real" pixel values. The MSE represents the mean of the "error" squares between the current picture and the bright image. The mistake is that the original image's values are different from the deteriorated image. Mean square error is given by:

$$MSE = \frac{\sum_{(i,j)} [f(i,j) - F(i,j)]^2}{N^2} \quad RMSE = \sqrt{MSE} \quad (4.3)$$

where f is the original image and F is the de-noised image and N is the size in pixel of the image.

4.4.3 Peak-Signal-to-Noise-Ratio

The PSNR gives the proportion of likely sign capacity to the force of the defiling clamor in the image. The term 'top sign to-clamor' signifies the greatest sign (power) proportion that influences its productivity and contortion of the commotion. As many signs have an exceptionally wide scope of elements (connection between the greatest and littlest potential upsides of an evolving amount), the logarithmic decibel size of the PSNR is commonly utilized. The right picture network and the debased picture framework aspects should be something similar. PSNR is set to:

$$PSNR = 20 \log_{10}((MAX)^2 / MSE), \quad (4.4)$$

where MAX represents the maximum signal value that exists in our original image. The higher the PSNR is the lower the noise in the image is, which implies a higher image quality image.

4.5 Image Contrast Change

Image contrast is the percentage of intensity changes in global image contrast, ΔC . Contract changes caused by filtering is defined as: the difference in mean intensity between the myocardial and blood pool regions, which is calculated as follows:

$$\Delta C = \left[\frac{\mu_f^{my} - \mu_f^{bp}}{\frac{1}{N} \sum_{i=1}^N (\mu_i^{my} - \mu_i^{bp})} - 1 \right] * 100 \quad (4.5)$$

where μ_f^{my} and μ_f^{bp} represent the mean strength value in the myocardial and blood-pool regions manually selected after filtering.; μ_i^{my} and μ_i^{bp} denote the mean intensity before filtering, the value N represents the total number of source single-view images; m represents the i the image and f denotes the filtered image.

4.5.1 Contrast-to-Noise-Ratio:

The percentage change in CNR, ΔCNR , caused by filtering is defined as:

$$\Delta CNR = \left[\frac{CNR_f}{\frac{1}{N} \sum_{m=1}^N CNR_i} - 1 \right] * 100 \quad (4.6)$$

whereas the CNR for the filtered image (f) or the m^{th} single-view image is computed as:

$$CNR = \frac{\mu^{my} - \mu^{bp}}{\sqrt{(\sigma^{my})^2 + (\sigma^{bp})^2}} \quad (4.7)$$

where μ refers to the default picture area deviation.

4.6 Comparison Between the Four Algorithms

We will now take a look at the results of the variation of these metrics for the THREE filters presented in this research. For the purpose of performance evaluation, we only consider a region of interest of size 6x5 in both the myocardial and blood pool region for the SNR, Contrast changes, and CNR values as shown in the Figure 4.8. One can see in Table 4.1 the estimated RMSE, PSNR, SNR, Contrast, and CNR of the region of interest without filtering. Table 4.2 and Table 4.3 show the same metrics for the Gaussian filter and the median filters for various σ and window size values. As expected, most metrics deteriorate as a function of σ for the Gaussian filter case and as a function of window size for the median filter case. This is due to the fact that the filters cannot adapt to local variation common when speckle noise is present.

Table 0.1. Metrics values for Noisy Image

RMSE	PSNR	SNR	Contrast	CNR
34.7870	17.3025	2.0917	1.771	0.0047

Table 0.2. Metrics values for Gaussian filtering with variable sigma.

Parameter - Sigma	RMSE	PSNR	SNR	Contrast	CNR
$\sigma = 1$	41.9413	15.6780	0.0074	0.0197	1.1704e-05
$\sigma = 1.5$	41.9489	15.6764	0.0100	0.0213	1.2392e-05
$\sigma = 2$	41.9665	15.6728	0.0119	0.0219	1.2953e-05
$\sigma = 3$	41.9644	15.6732	0.0138	0.0226	1.3176e-05
$\sigma = 5$	41.9916	15.6676	0.0162	0.0236	1.3311e-05

Table 0.3. Metrics values for Median filtering with variable sigma

Parameter - Window	RMSE	PSNR	SNR	Contrast	CNR
$\sigma = 1$	25.7879	19.9025	1.6491	1.9239	0.0040
$\sigma = 1.5$	26.0949	19.7997	1.3072	2.0867	0.0033
$\sigma = 2$	26.6714	19.6099	1.1437	2.2495	0.0029
$\sigma = 3$	27.0229	19.4962	0.9793	2.3686	0.0026
$\sigma = 5$	29.3685	18.7732	0.8203	2.4483	0.0023

Table 4.4. Metrics values for Anisotropic Geodesic with variable sigma; window size=3x3

Parameter	RMSE	PSNR	SNR	Contrast	CNR
$\sigma = 1.5$	35.5443	17.1154	4.4659	2.0808	0.0059
$\sigma = 2$	36.5636	16.8698	3.9210	2.2084	0.0054
$\sigma = 3$	37.0061	16.7653	3.7597	2.3980	0.0049
$\sigma = 5$	37.4865	16.6533	3.6804	2.4517	0.0047

$\sigma = 7$	37.7554	16.5912	3.3045	2.4903	0.0044
--------------	---------	---------	--------	--------	--------

Table 4.5. Metrics values for Anisotropic Geodesic with variable sigma; window size =11x11

Parameter - Sigma	RMSE	PSNR	SNR	Contrast	CNR
$\sigma = 1.5$	69.6833	11.2570	0.0809	0.0297	2.9220e-05
$\sigma = 2$	69.7171	11.2753	0.0726	0.257	2.9474e-05
$\sigma = 3$	69.7589	11.2691	0.0834	0.0361	2.3383e-05
$\sigma = 5$	69.8462	11.2223	0.1272	0.399	2.3453e-05
$\sigma = 7$	69.9521	11.1848	0.2421	0.4471	2.3731e-05

This filter has numerous potential applications in medical imaging and image processing. Its applications are not just limited to medical and medicine field but can also be used to suppress speckle noise from SAR images as well. In case of ultrasound, it can be used to improve surgical guidance and robotic-assisted interventions which necessitate high quality images where the filtering can be embedded directly in the ultrasound machine.

4.7 Discussion:

In this work, we were able to demonstrate that by adapting a non-linear filter developed to process range images, we were able to filter multiplicative noise in ultrasound images. This filter called anisotropic geodesic filter possess similar quality as the well-known anisotropic gradient-based filter from Perona-Malik but do not require to compute image gradients and is free of non-intuitive parameters like integration time and diffusion coefficient. The filter can be easily generalized to any complex signals such as colour range images, MRI, CT etc. One of the key properties of this algorithm is its ability to filter continuous regions without the loss of localization of important features. This is a key property for medical applications. The filter is akin to a Gaussian filter in continuous regions and responds like an anisotropic filter in regions with sharp discontinuities. Experimental comparisons with two of the most well-known filters were able to demonstrate its superior capability at filtering ultrasound images.

CHAPTER FIVE

CONCLUSION AND FUTURE WORKS

5.1 Conclusions

In this thesis, we have demonstrated that by adapting a non-linear filter developed to process a range of images, we are able to filter multiplicative noise in ultrasound images. This filter called anisotropic geodesic filter possess similar quality as the well-known anisotropic gradient-based filter from Perona-Malik but do not require to compute image gradients and is free of non-intuitive parameters like integration time and diffusion coefficient. The filter can be easily generalized to any complex signals such as colour range images, MRI, CT etc. One of the key properties of this algorithm is its ability to filter continuous regions without the loss of localization of important features. This is a key property for medical applications. The filter is akin to a Gaussian filter in continuous regions and responds like an anisotropic filter in regions with sharp discontinuities. Experimental comparisons with two of the most well-known filters were able to demonstrate its superior capability at filtering ultrasound images.

This filter has numerous potential applications in medical imaging and image processing. Its applications are not just limited to medical and medicine field but can also be used to suppress speckle noise from SAR images as well. In case of ultrasound, it can be used to improve surgical guidance and robotic-assisted interventions which necessitate high quality images where the filtering can be embedded directly in the ultrasound machine.

5.2 Future Works

The proposed filter is application specific and can be further generalized for different types of imaging applications. For instance:

- Instead of using a 2-D manifold immersed in an N-D space one could easily generalize the approach to a 3-D or even 4-D manifold immersed in an N-D space. This will allow to process volumetric not only at the slice level but truly at the voxel level for the 3-D case and time varying voxels in the 4-D case;
- Using this framework, one could filter not only CT and MRI but also, with a 4-D framework, real-time cardiac MR data;
- This would require to generalize our Single Source Shortest Path (SS-SP) algorithm to the 3-D and 4-D cases;
- Real-time implementation of the SS-SP algorithm using GPU could be done in order to achieve real-time performance;

- Other medical imaging modalities such as CT, MRI and multi-view ultrasound can be incorporated by applying the filter as a pre-processing step to smooth out 2-D and 3-D images while preserving the fine features of the image such as edges;

- The method can be further extended to multi-spectral images.



REFERENCES

- Aditi Gupta, Vikrant Bhateja, Avantika Srivastava, Ananya Gupta. (2018). Speckle Noise Suppression in Ultrasound Images by Using an Improved Non-local Mean Filter: Proceedings of ICSCSP. Soft Computing and Signal Processing (pp.13-19)
- Afsham, N., Rasoulia, A., Najafi, M., Abolmaesumi, P., & Rohling, R. (2015). Nonlocal means filter-based speckle tracking. *IEEE transactions on ultrasonics, ferroelectrics, and frequency control*, 62(8), 1501-1515.
- Andria, G., Attivissimo, F., Lanzolla, A. M., & Savino, M. (2013). A suitable threshold for speckle reduction in ultrasound images. *IEEE Transactions on instrumentation and measurement*, 62(8), 2270-2279.
- Aravind B. N; K. V. Suresh. (2015) An improved image denoising using wavelet transform. In *2015 International Conference on Trends in Automation, Communications and Computing Technology (I-TACT-15)* (pp. 1-5).
- Chen, P. Y., & Lien, C. Y. (2008). An efficient edge-preserving algorithm for removal of salt-and-pepper noise. *IEEE Signal Processing Letters*, 15, 833-836.
- Eslami, R., & Radha, H. (2007). A new family of nonredundant transforms using hybrid wavelets and directional filter banks. *IEEE Transactions on image processing*, 16(4), 1152-1167.
- Farouj, Y., Karahanoğlu, F. I., & Van De Ville, D. (2017). Regularized spatiotemporal deconvolution of fMRI data using gray-matter constrained total variation. *IEEE 14th International Symposium on Biomedical Imaging* (pp. 472-475).
- Franceschi A. M, and Rosenkrantz A. B. (2017) Patterns of recent national institutes of health (NIH) funding to diagnostic radiology departments. *Academic Radiology*, pages 1076–6332.
- Gravel P., Beaudoin G., De Guise, J. A. (2004). A method for modeling noise in medical images. *IEEE Transactions on medical imaging*, 23(10), 1221-1232.
- GreeksforGreeks, (2021) Available in: <https://www.geeksforgeeks.org/graph-data-structure-and-algorithms/?ref=lbp#shortestPath>
- Gupta, D., Anand, R. S., & Tyagi, B. (2015). Speckle filtering of ultrasound images using a modified non-linear diffusion model in non-subsampled shearlet domain. *IET Image Processing*, 9(2), 107-117.

- Hongga Li, Bo Huang, Xiaoxia Huang. (2010). A Level Set Filter for Speckle Reduction in SAR Images. *EURASIP Journal on Advances in Signal Processing*.
- Huo, Q., Li, J., Lu, Y., & Yan, Z. (2016). Removing ring artifacts in CBCT images via smoothing. *International Journal of Imaging Systems and Technology*, 26(4), 284-294.
- Ioannidou, S., & Karathanassi, V. (2007). Investigation of the dual-tree complex and shift-invariant discrete wavelet transforms on Quickbird image fusion. *IEEE geoscience and remote sensing letters*, 4(1), 166-170.
- Iqbal, M. Z., Ghafoor, A., & Siddiqui, A. M. (2012). Satellite image resolution enhancement using dual-tree complex wavelet transform and nonlocal means. *IEEE geoscience and remote sensing letters*, 10(3), 451-455.
- J. S. Lee, L. Jurkevich, P. Dewaele, P. Wambacq, A. Oosterlinckm, (2009) Speckle filtering of synthetic aperture radar images: A review, *Remote Sensing Reviews*.
- Jing Bianca S. Gerendas Christian Simader Georg Langs Sebastian M. Waldstein Ursula Schmidt-Erfurth Ehsan Shahrian Varnousfaderani, Wolf-Dieter Vogl. (2016) Geodesic denoising for optical coherence tomography images, *Proc. SPIE 9784, Medical Imaging: Image Processing*.
- Khalid Youssef, Nanette N Jarenwattananon, Louis-S Bouchard. (2015) Feature-preserving noise removal. *IEEE Transactions on Medical Imaging*, 34(9), 1822-1829.
- Kim, D., Ramani, S., & Fessler, J. A. (2014) Combining ordered subsets and momentum for accelerated X-ray CT image reconstruction. *IEEE transactions on medical imaging*, 34(1), 167-178.
- Lifeng Yu, Mayo Clinic, Rochester, Shuai Leng, (2016). Image Reconstruction Techniques, *Image Wisely Files - Medical-Physicist-Articles*.
- Lopes A., Nezry E, Touzi R., and H. Laur. (1990). Maximum a posteriori speckle filtering and first order texture models in SAR images. *In 10th Annual International Symposium on Geoscience and Remote Sensing*, pp. 2409–2412.
- Mathew K., Shibu S. (2014) Reconstruction of Wavelet Coefficients. *International Journal of Computer Applications (0975 – 8887)*, Volume 97– No.15.
- Michailovich, O. V., Tannenbaum A. (2006). Despeckling of medical ultrasound images. *IEEE Transactions on Ultrasonics, Ferroelectrics, And Frequency Control*, 53(1), 64-78.

- Mohammad Ashraful Islam, Rafid Mostafiz, Mithun Kumar PK, Mohammad Motiur Rahman (2018) Speckle noise reduction for 3D ultrasound images by optimum threshold parameter estimation of bi-dimensional empirical mode decomposition using Fisher discriminant analysis. *International Journal of Signal and Imaging Systems Engineering* 11(2):93.
- Nikpour, M., & Hassanpour, H. (2010). Using diffusion equations for improving performance of wavelet-based image denoising techniques. *IET Image Processing*, 4(6), 452-462.
- Noor H. Resham, Heba Kh. Abbas, Haidar J. Mohamad, Anwar H. Al-Saleh (2021) Noise Reduction, Enhancement and Classification for Sonar Images, *Iraqi Journal of Science*, Vol. 62, No. 11(Special Issue), pp: 4439-4452.
- Palwinder Singh, Leena Jain. (2013). Noise reduction in ultrasound images using wavelet and spatial filtering techniques. *IEEE 2nd International Conference on Information Management in the Knowledge Economy.*, pages 57–63.
- Patel, B. C., Sinha, G. R. (2014). Abnormality detection and classification in computer-aided diagnosis (CAD) of breast cancer images. *Journal of Medical Imaging and Health Informatics*, 4(6), 881-885.
- Perona, P., Malik, J. (1990). Scale-space and edge detection using anisotropic diffusion. IEEE Computer Society, *IEEE Trans. Pattern Anal. Mach. Intell.*, Vol 12(7): pp. 629– 639.
- Piotr Osinski, Jakub Markiewicz, Jarosław Nowisz, Michał Remiszewski, Albert Rasiński and Robert Sitnik. (2022) A Novel Approach for Dynamic (4d) Multi-View Stereo System Camera Network Design. *MPDI, Sensors Journal*.
- Prentice Hall, Inc, Upper Saddle River, NJ.*
- Rafael, C. Gonzalez and Richard, E. Woods. (2002) Digital Image Processing. 2nd Edition
- Ranjani, J. J., & Chithra, M. S. (2015). Bayesian denoising of ultrasound images using heavy-tailed Levy distribution. *IET Image Processing*, 9(4), 338-345.
- Ranjani, J. J., & Thiruvengadam, S. J. (2010). Dual-tree complex wavelet transform based SAR despeckling using interscale dependence. *IEEE Transactions on geoscience and remote sensing*, 48(6), 2723-2731.
- S. Di Zenzo, “A note on the gradient of a multi-image,” *Computer Vision, Graphics and Image Processing*, pp. 402–407, 1986.

- S. Hariharasudhan and Dr. B. Raghu. (2016) A Virtual Analysis on Effective Speckle Noise Removal Techniques in Medical Images by Various Filtering Methods, *volume V38(3). Seventh Sense Research Group.*
- Sapthagirivasan, V., & Mahadevan, V. (2010). Denoising and fissure extraction in high resolution isotropic CT images using Dual Tree Complex Wavelet Transform. *2nd International Conference on Software Technology and Engineering* (Vol. 1, pp. V1-362).
- Sixin Zhang, Stéphane Mallat. (2021) Maximum Entropy Models from Phase Harmonic Covariances. *Hal And Open Science.*
- Xu, X., Cao, X., & Zhao, L. (2013). Comparison of rice husk-and dairy manure-derived biochars for simultaneously removing heavy metals from aqueous solutions: role of mineral components in biochars. *Chemosphere*, 92(8), 955-961.
- Yan F. X., Peng S. L., Cheng, L. Z. (2007). Dual-tree complex wavelet hidden Markov tree model for image denoising. *Electronics Letters*, 43(18), 973-975.
- Yao Zhang, Heng Xue, Mixue Wang, Nan He, Zhibin Lv, Ligang Cui (2021) Lung ultrasound findings in patients with coronavirus disease (COVID-19). *American Journal of Roentgenology*, 216(1), 80-84.
- Yi-Sheng Sun, Zhao Zhao, Zhang Yang, Fang Xu, Hang-Jing Lu, Zhi-Yong Zhu, Wen Shi, Jianmin Jiang, Ping-Ping Yao, Han-Ping Zhu. (2017) Risk factors and preventions of breast cancer. *International journal of biological sciences*, 13(11), 1387.
- Dr Saad, Zidan, Baqubah Hospital, Diyala, (2021).